INTERNATIONAL JOURNAL FOR NUMERICAL METHODS IN FLUIDS
Int. J. Numer. Meth. Fluids 2005; **48**:947–983
Published online 31 March 2005 in Wiley InterScience (www.interscience.wiley.com). DOI: 10.1002/fld.969

Numerical solution of the Boltzmann equation by time relaxed Monte Carlo (TRMC) methods

Lorenzo Pareschi*,† and Stefano Trazzi‡

Department of Mathematics, University of Ferrara, Via Machiavelli 35, I-44100 Ferrara, Italy

SUMMARY

A new family of Monte Carlo schemes has been recently introduced for the numerical solution of the Boltzmann equation of rarefied gas dynamics (*SIAM J. Sci. Comput*. 2001; **23**:1253–1273). After a splitting of the equation the time discretization of the collision step is obtained from the Wild sum expansion of the solution by replacing high-order terms in the expansion with the equilibrium Maxwellian distribution. The corresponding time relaxed Monte Carlo (TRMC) schemes allow the use of time steps larger than those required by direct simulation Monte Carlo (DSMC) and guarantee consistency in the fluid-limit with the compressible Euler equations. Conservation of mass, momentum, and energy are also preserved by the schemes. Applications to a two-dimensional gas dynamic flow around an obstacle are presented which show the improvement in terms of computational efficiency of TRMC schemes over standard DSMC for regimes close to the fluid-limit. Copyright © 2005 John Wiley & Sons, Ltd.

KEY WORDS: Boltzmann equation; Monte Carlo methods; time relaxed schemes; fluid-dynamic limit; Euler equations; stiff systems

1. INTRODUCTION

The mathematical model we consider is the kinetic Boltzmann equation for rarefied gas dynamics (RGD) which characterizes the temporal evolution of a particle density function $f(x, v, t)$ according to

$$\frac{\partial f}{\partial t} + v \cdot \nabla_x f = \frac{1}{\varepsilon} Q(f, f), \quad x \in \Omega \subset \mathbb{R}^3, \ \ v \in \mathbb{R}^3 \tag{1}$$

*Correspondence to: Lorenzo Pareschi, Department of Mathematics, University of Ferrara, Via Machiavelli 35, I-44100 Ferrara, Italy.
†E-mail: pareschi@dm.unife.it
‡E-mail: trazzi@dm.unife.it

Contract/grant sponsor: EC; contract/grant number: HPRN-CT-2002-00282

Received 23 February 2004
Revised 19 January 2005
Accepted 21 January 2005

supplemented with the initial condition

$$f(x, v, t=0) = f_0(x, v) \tag{2}$$

The non-negative density function f depends on position $x \in \mathbb{R}^3$, velocity $v \in \mathbb{R}^3$ and time $t > 0$ and can depend on other independent variables like an internal energy [1].

In (1) the parameter $\varepsilon > 0$ is called *Knudsen number* and it is proportional to the mean free path between collisions. The bilinear collisional operator $Q(f, f)$ which describes the binary collisions between particles in a mono-atomic gas is given by

$$Q(f, f)(v) = \int_{\mathbb{R}^3} \int_{S^2} \sigma(|v - v_*|, \omega)(f(v')f(v'_*) - f(v)f(v_*)) \, \mathrm{d}\omega \, \mathrm{d}v_* \tag{3}$$

where for simplicity the dependence of f on x and t has been omitted.

In the previous expression ω is a vector of the unitary sphere $S^2 \subset \mathbb{R}^3$. The collisional velocities (v', v'_*) are associated to the velocities (v, v_*) and to the parameter ω by the relations

$$v' = \tfrac{1}{2}(v + v_* + |q|\omega), \quad v'_* = \tfrac{1}{2}(v + v_* - |q|\omega) \tag{4}$$

where $q = v - v_*$ is the relative velocity.

The kernel σ is a non-negative function which characterizes the details of the binary interaction between particles. In the case of a kth power forces inversely proportional to the distance between particles, the kernel is

$$\sigma(|q|, \theta) = b_\alpha(\theta)|q|^\alpha \tag{5}$$

where $\alpha = (k-5)/(k-1)$ and θ is the scattering angle between q and $|q|\omega$. The *variable hard sphere* (VHS) model is often used in numerical simulation of rarefied gases, and consists in choosing $b_\alpha(\theta) = C_\alpha$ with C_α a positive constant. The case $\alpha = 0$ corresponds to a *Maxwellian gas*, while $\alpha = 1$ is called a *hard sphere gas*.

In this paper we consider the multidimensional extension of the time relaxed Monte Carlo (TRMC) methods recently introduced in Reference [2] and present a numerical comparison with a classical direct simulation Monte Carlo (DSMC). Since TRMC methods are based on a suitably time discretized Boltzmann equation we use as a DSMC comparison the time discrete Nanbu–Babovsky (NB) [3, 4] method instead of Bird's method [5].

Let us recall that the main difference between Bird and NB methods is that in NB scheme particles can collide only once per time step, while in Bird's scheme multiple collisions are allowed. This has a profound influence on the time accuracy of the methods as well as on their mathematical analysis. In fact, while the solution of the NB scheme converges in probability to the solution of the time discrete Boltzmann equation [6], Bird's method converges to the solution of the time continuous Boltzmann equation [7].

A modified version of TRMC which avoids the introduction of a time discretization error and which is based on a recursive strategy has been recently presented in Reference [8]. A comparison of the recursive TRMC method with Bird's algorithm is actually under development [9] and will be presented elsewhere.

The goal of TRMC methods is to construct simple and efficient numerical methods for the solution of the Boltzmann equation in regions with a large variation of the mean free path [2, 10–13]. These methods are based on a splitting of the Boltzmann equation and on a time discretization of the collision step [2, 14], which is robust in the fluid-limit.

As a consequence the resulting TRMC methods have the following features:

- For large Knudsen numbers, the TRMC method behaves as a classical DSMC method. In particular the sampling of new colliding particles is the same as in classical DSMC methods.
- In the limit of the very small Knudsen number, the collision step replaces the distribution function by a local Maxwellian with the same moments. The TRMC method will behave as a stochastic kinetic scheme for the underlying Euler equations of gas dynamics [15].
- Mass, momentum, and energy are preserved.

Previous techniques for acceleration of DSMC close to fluid regimes, such as [16–19], have divided the spatial region into two subregions: a fluid region in which the Euler or Navier–Stokes equations are solved and an RGD region in which DSMC is used. The focus of these methods has been to determine how best to choose the two domains and on design of boundary conditions to couple the fluid and RGD regions. These coupling methods have proved to be very useful, but they are still limited by their performance close to fluid regions, where DSMC is slow but the fluid equations are inaccurate. In References [20, 21] an adaptive mesh refinement strategy has been included into DSMC to overcome some of the problems introduced by small Knudsen numbers. We see these approaches as complementary strategies to the unified TRMC approach. For example to improve coupling based methods, it may make sense to use a TRMC-like method in a near continuum region between the pure fluid and pure DSMC regions.

After this introduction we will recall some basic facts about the Boltzmann equation and its fluid-dynamic limit. Next in Section 3 we will discuss the problem of the time discretization of the Boltzmann equation. Section 4 is devoted to a short description of the different Monte Carlo methods. Finally, in the last section we present the detailed numerical results of the simulation of a two-dimensional flow around an ellipse for several values of the mean free path. The results show a marked improvement in the efficiency of computations given by TRMC for small Knudsen numbers.

2. PHYSICAL BACKGROUND

2.1. Collisional invariants and the Euler equations

Let f and ϕ be such that $\int_{\mathbb{R}^3} Q(f,f)\phi(v)\,\mathrm{d}v$ exists. Then it is possible to show the identity

$$\int_{\mathbb{R}^3} Q(f,f)\phi(v)\,\mathrm{d}v = \frac{1}{2}\int_{\mathbb{R}^3}\int_{\mathbb{R}^3}\int_{S^2} f' f'_*(\phi' + \phi'_* - \phi - \phi_*)\sigma(|q|,\omega)\,\mathrm{d}v\,\mathrm{d}v_*\,\mathrm{d}\omega \tag{6}$$

where $f' = f(x, v', t)$, $f'_* = f(x, v'_*, t)$.

If ϕ is such that

$$\phi + \phi_* = \phi' + \phi'_*$$

then the previous integral vanishes independently from the function f.

More precisely $\phi(v)$ is a linear combination of the elementary collisional invariants $1, v, |v|^2$, which corresponds to the conservation of mass ρ, momentum ρu and energy E

$$\rho = \int_{\mathbb{R}^3} f \, \mathrm{d}v, \quad \rho u = \int_{\mathbb{R}^3} f v \, \mathrm{d}v, \quad E = \frac{1}{2} \int_{\mathbb{R}^3} f |v|^2 \, \mathrm{d}v \tag{7}$$

The gas temperature is then recovered as

$$T = \frac{1}{3\rho} \int_{\mathbb{R}^3} f(v-u)^2 \, \mathrm{d}v = \frac{1}{3\rho} (2E - u^2) \tag{8}$$

Now, if we consider the Boltzmann equation (1) and multiply it for $1, v, |v|^2$ by integrating in v we obtain

$$\frac{\partial \rho}{\partial t} + \sum_{i=1}^{3} \frac{\partial}{\partial x_i} (\rho u_i) = 0 \tag{9}$$

$$\frac{\partial}{\partial t}(\rho u_j) + \sum_{i=1}^{3} \frac{\partial}{\partial x_i} (\rho u_i u_j + p_{ij}) = 0, \quad j = 1,2,3 \tag{10}$$

$$\frac{\partial}{\partial t} \left(\frac{1}{2} \rho |u|^2 + \rho e \right) + \sum_{i=1}^{3} \frac{\partial}{\partial x_i} \left[\rho u_i \left(\frac{1}{2} |u|^2 + e \right) + \sum_{j=1}^{3} u_i p_{ij} + q_i \right] = 0 \tag{11}$$

These equation are the corresponding conservation laws for mass, momentum and energy. Unfortunately the differential equations system is not closed, since it involves higher order moments of the density function f.

Taking $\phi = \log(f)$ in (6) it is easy to show that the collisional operator is such that the *H-Theorem* holds

$$\int_{\mathbb{R}^3} Q(f,f) \log(f) \, \mathrm{d}v \leqslant 0 \tag{12}$$

This condition implies that each function f in equilibrium (i.e. $Q(f,f) = 0$) has locally the form of a Maxwellian distribution

$$M(\rho, u, T)(v) = \frac{\rho}{(2\pi T)^{3/2}} \exp\left(-\frac{|u-v|^2}{2T} \right) \tag{13}$$

Formally as $\varepsilon \to 0$ the function f is locally replaced by a Maxwellian. In this case it is possible to compute f from its moments thus obtaining the closed Euler system of compressible gas dynamics

$$\begin{gathered} \frac{\partial \rho}{\partial t} + \nabla_x \cdot (\rho u) = 0 \\ \frac{\partial (\rho u)}{\partial t} + \nabla_x \cdot (\rho u \otimes u + p) = 0 \\ \frac{\partial E}{\partial t} + \nabla_x \cdot (Eu + pu) = 0 \end{gathered} \tag{14}$$

$$p = \rho T, \quad E = \tfrac{3}{2} \rho T + \tfrac{1}{2} \rho |u|^2$$

More in general using for small values of ε the Chapman–Enskog expansion

$$f = M + \varepsilon f_1 + \varepsilon^2 f_2 + \cdots + \varepsilon^n f_n$$

it is possible to obtain the compressible Navier–Stokes equations (at the order $n=1$) and going further the Burnett system (at the order $n=2$). We refer to Cercignani [1] for more details.

2.2. *Boundary conditions*

Typically, Equation (1) is completed with boundary conditions for $x \in \partial\Omega$. The boundary conditions for mono-atomic gases are described by

$$|v \cdot n(x)| f(x,v,t) = \int_{v' \cdot n(x) < 0} |v' \cdot n(x)| K(x, v' \longrightarrow v, t) f(x, v', t)\, \mathrm{d}v' \tag{15}$$

where $n(x)$ is the inner normal vector in x of $\partial\Omega$ and the entering flux is described by the outgoing one modified by the kernel K. Such definition of the boundary conditions preserve the mass if

$$K(x, v' \longrightarrow v, t) \geqslant 0, \quad \int_{v \cdot n(x) \geqslant 0} K(x, v' \longrightarrow v, t)\, \mathrm{d}v = 1 \tag{16}$$

The conditions most used are the Maxwellian ones, in which particles that collide with a surface are remitted in local equilibrium with the same temperature of the object. This is just an approximation of the true physical behaviour. More accurate descriptions are obtained if a fraction α is absorbed by the obstacle and remitted with the object temperature, while the remaining part $1-\alpha$ is completely reflexed

$$f(x,v,t) = (1-\alpha) Rf(x,v,t) + \alpha M f(x,v,t), \quad x \in \partial\Omega, \quad v \cdot n(x) \geqslant 0 \tag{17}$$

where

$$Rf(x,v,t) = f(x, v - 2n(x)(n(x) \cdot v), t) \tag{18}$$

$$Mf(x,v,t) = \eta(x,t) M_\omega(v) \tag{19}$$

If T_ω is the object temperature, then M_ω is determined by

$$M_\omega = \exp\left(-\frac{v^2}{2T_\omega}\right)$$

while η is given by the conservation of the mass at the surface of the object

$$\eta(x,t) \int_{v \cdot n(x) \geqslant 0} M_\omega(v) |v \cdot n(x)|\, \mathrm{d}v = \int_{v \cdot n(x) < 0} f(x,v,t) |v \cdot n(x)|\, \mathrm{d}v \tag{20}$$

The coefficient α, with $0 \leqslant \alpha \leqslant 1$ is called *absorption coefficient*. Diffusion with total absorption by the surface ($\alpha = 1$) is the classical model used to describe the behaviour of a mono-atomic gas, since α has been experimentally estimated to be close to 1.

3. TIME RELAXED SCHEMES

The time integration of the Boltzmann equation represents a challenging problem, since the nonlinear collision operator becomes highly stiff near the fluid regime ($\varepsilon \ll 1$). An additional limitation is given by the high computational cost required for evaluating the fivefold collisional integral.

3.1. Time discretizations of the Boltzmann equation

The starting point is the usual first order splitting in time of (1), which consists of solving separately a purely convective step (i.e. $Q \equiv 0$ in (1)) and a collision step characterized by a space homogeneous Boltzmann equation (i.e. $\nabla_x f \equiv 0$ in (1)). Clearly, after this splitting, almost all the main difficulties are contained in the collision step. For this reason, in what follows we will fix our attention on the time discretization of the homogeneous Boltzmann equation

$$\frac{\partial f}{\partial t} = \frac{1}{\varepsilon} Q(f, f) \tag{21}$$

For example, let us consider the simple forward Euler scheme

$$f^{n+1} = f^n + \frac{\Delta t}{\varepsilon} Q(f^n, f^n) \tag{22}$$

which has been widely used in simulation. It leads to a stability condition which requires the time step Δt to be of order ε. Thus for small values of ε the scheme is unusable for practical purposes. Clearly better stability properties can be obtained using fully implicit schemes. However the computational difficulties related with the implicit evaluation of $Q(f, f)$ make this alternative unpracticable.

3.2. Wild sums and time relaxed discretizations

As proposed in Reference [14], a general idea for deriving robust numerical schemes, that is, schemes that are unconditionally stable and preserve the asymptotic of the fluid-dynamic limit, for a nonlinear equation like (21), is to replace high-order terms of a suitable well-posed power series expansion by the local equilibrium. Here we briefly recall the schemes. For more details we refer the reader to References [10, 14].

Let us consider a differential system of the type

$$\frac{\partial f}{\partial t} = \frac{1}{\varepsilon} [P(f, f) - \mu f] \tag{23}$$

with the same initial condition (2), and where $\mu \neq 0$ is a constant and P a bilinear operator.

Now, the solution to the Cauchy problem for (23) can be expressed in the form of a power series

$$f(v,t) = \mathrm{e}^{-\mu t/\varepsilon} \sum_{k=0}^{\infty} (1 - \mathrm{e}^{-\mu t/\varepsilon})^k f_k(v) \tag{24}$$

where the functions f_k are given by the recurrence formula

$$f_{k+1}(v) = \frac{1}{k+1} \sum_{h=0}^{k} \frac{1}{\mu} P(f_h, f_{k-h}), \quad k = 0, 1, \ldots \tag{25}$$

The method was originally developed by Wild [22] and Carlen *et al.* [23] to solve the Boltzmann equation for Maxwellian molecules. In Reference [14], the method has been extended to take into account more general hypothesis on P. In the case of the Boltzmann equation, that is $P(f, f) = Q(f, f) + \mu f$ formally we have that

$$\lim_{k \to \infty} f_k(v) = \lim_{t \to \infty} f(v, t) = M(v)$$

where $M(v)$ is the local Maxwellian equilibrium.

Using this remark, in Reference [14], the following class of numerical schemes, based on a Maxwellian truncation for $m \geqslant 1$ of (24), has been constructed

$$f^{n+1}(v) = \mathrm{e}^{-\mu \Delta t/\varepsilon} \sum_{k=0}^{m} (1 - \mathrm{e}^{-\mu \Delta t/\varepsilon})^k f_k^n(v) + (1 - \mathrm{e}^{-\mu \Delta t/\varepsilon})^{m+1} M(v) \tag{26}$$

where $f^n = f(n\Delta t)$ and Δt is a small time interval. It can be shown that the schemes obtained in this way are of order m in time.

Furthermore, we have [14] the following properties for $P(f, f) = Q(f, f) + \mu f$:

(i) *Conservations*:

$$\int_{\mathbb{R}^3} P(f, f) \phi(v) \, \mathrm{d}v = \mu \int_{\mathbb{R}^3} f \phi(v) \, \mathrm{d}v \tag{27}$$

and

$$\int_{\mathbb{R}^3} f^{n+1} \phi(v) \, \mathrm{d}v = \int_{\mathbb{R}^3} f^n \phi(v) \, \mathrm{d}v \tag{28}$$

for $\phi(v) = 1, v, |v|^2$.

(ii) *Asymptotic preservation* (AP):

For any $m \geqslant 1$, we have

$$\lim_{\mu \Delta t/\varepsilon \to \infty} f^{n+1} = M(v) \tag{29}$$

In the case of the Boltzmann equation if we denote by $Q_{\bar{\sigma}}(f, f)$ the collision operator where the collision kernel σ has been replaced by the bounded one $\sigma_{\bar{\sigma}}(v, v_*) = \max\{\sigma(v, v_*), \bar{\sigma}\}$, where $\bar{\sigma} > 0$ is a constant, we have

$$P_{\bar{\sigma}}(f, f) = Q_{\bar{\sigma}}(f, f) + \mu f \geqslant 0$$

for $\mu = 4\pi\bar{\sigma}\rho$.

Under this assumption, which is numerically essential, the solution provided by TR schemes is also non negative.

Remark 3.1
We point out that for $m=0$ TR schemes are equivalent to the exact solution in a time step Δt of the space homogeneous BGK approximation of the Boltzmann equation.

Remark 3.2
The method described can be generalized by using different weight function, with the goal of finding a best approximation for the highest order coefficients of Wild sum expansion (24).

In general this schemes can be written in the form

$$f^{n+1} = \sum_{k=0}^{m} A_k f_k + A_{m+1} M \tag{30}$$

where the coefficient f_k are determined by (25).

The weights $A_k = A_k(t)$ are not negative functions which satisfy

(i) *Consistency*:

$$\lim_{\tau\to 0} A_1(\tau)/\tau = 1, \quad \lim_{\tau\to 0} A_k(\tau)/\tau = 0, \quad k = 2,\ldots,m+1 \tag{31}$$

(ii) *Conservations*:

$$\sum_{k=0}^{m+1} A_k = 1, \quad \tau \in [0,1] \tag{32}$$

(iii) *Asymptotic preservation* (AP):

$$\lim_{\tau\to 1} A_k(\tau) = 0, \quad k = 0,\ldots,m \tag{33}$$

A possible choice of function satisfying the above conditions is

$$A_k = (1-\tau)\tau^k, \quad k = 0,\ldots,m, \quad A_{m+1} = \tau^{m+1} \tag{34}$$

which correspond to scheme (26).

A better choice of parameter has been presented in Reference [10]

$$A_k = (1-\tau)\tau^k, \quad k = 0,\ldots,m-1 \tag{35}$$

$$A_m = 1 - \sum_{k=0}^{m} A_k - A_{m+1}, \quad A_{m+1} = \tau^{m+2} \tag{36}$$

that correspond to consider $f_{m+1} = f_m$, $f_k = M$, $k \geqslant m+2$ in (24).

We emphasize that other choices of parameters are possible, and the individuation of the optimal ones is an open problem. Some interesting results for Maxwellian molecules have been obtained recently in Reference [24].

4. TRMC METHODS

In this section, we describe the TRMC method for the evolution of the density function f. We shall include the description of the classical DSMC no-time counter algorithm, so that it will be easier to make a comparison between the new formulation and the previous one.

4.1. The Nanbu–Babovsky DSMC method

Here we will describe the classical DSMC method in the general framework we have introduced in the previous sections. More specifically, we consider the Nanbu–Babovsky algorithm [3, 4]. The convergence of this scheme has been proved by Babovsky and Illner [6].

In the sequel we will implicitly assume that the collision kernel in the Boltzmann equation has been replaced by the bounded one. For simplicity of notations we will omit the subscript $\bar{\sigma}$ when referring to $Q_{\bar{\sigma}}(f, f)$ and $P_{\bar{\sigma}}(f, f)$.

The Boltzmann equation can be written in the form

$$\frac{\partial f}{\partial t} = \frac{1}{\varepsilon}\left[P(f, f) - \mu f\right] \tag{37}$$

We assume that f is a probability density; i.e.

$$\rho = \int_{\mathbb{R}^3} f(v, t)\, \mathrm{d}v = 1$$

Let us discretize time and denote by $f^n(v)$ an approximation of $f(v, n\Delta t)$. The forward Euler scheme applied to (37) is written as

$$f^{n+1} = \left(1 - \frac{\mu \Delta t}{\varepsilon}\right) f^n + \frac{\mu \Delta t}{\varepsilon} \frac{P(f^n, f^n)}{\mu} \tag{38}$$

Note that for bounded collision kernels $P(f, f)/\mu \geqslant 0$ if $\mu = 4\pi\bar{\sigma}$ and thus by mass conservation is a probability density. Note also that $P(f, f)/\mu = f_1$ that is the first term in the Wild expansion.

Thus the equation has the following probabilistic interpretation. To sample one particle from f^{n+1}, with probability $(1 - \mu\Delta t/\varepsilon)$ we sample the particle from f^n and with probability $\mu\Delta t/\varepsilon$ we sample the particle from $P(f^n, f^n)(v)/\mu$.

We remark here that this probabilistic interpretation of (38) breaks down if $\Delta t/\varepsilon$ is too large because the coefficient of f^n on the right-hand side may become negative. This implies that the time step becomes extremely small when approaching the fluid-dynamic limit. Therefore Nanbu–Babowski method becomes almost unusable near the fluid regime. We refer to Reference [25] for a more detailed discussion on the time step limitations of standard DSMC methods.

The essential feature of the Monte Carlo method is the way particles are sampled from $P(f, f)/\mu$. This is done with the aid of an acceptance–rejection technique combined with a collision strategy of the samples. In its first version, Nanbu's algorithm was not conservative; i.e. energy and momentum were conserved only in the mean but not at each collision. A conservative version of the algorithm was introduced by Babovsky [4]. Instead of selecting

single particles, independent particle pairs are selected, and conservation is maintained at each collision.

The algorithm for evolving the density up to time $t = n_{\mathrm{TOT}}\Delta t$ is the following.

Algorithm 4.1 (*DSMC for VHS molecules*)

- *compute the initial velocity of the particles*, $\{v_i^0, i = 1, \ldots, N\}$, *by sampling them from the initial density* $f_0(v)$
- for $n = 1$ to n_{TOT}
  given $\{v_i^n, i = 1, \ldots, N\}$,
  - *compute an upper bound* $\bar{\sigma}$ *for the cross-section*
  - *set* $\mu = 4\pi\bar{\sigma}$
  - *set* $N_c = \mathrm{Iround}(\mu N \Delta t/(2\varepsilon))$
  - *select* N_c *dummy collision pairs* (i, j) *uniformly among all possible pairs, and for those*
    - *compute the relative cross-section* $\sigma_{ij} = \sigma(|v_i - v_j|)$
    - if $\bar{\sigma}\,\mathrm{Rand} < \sigma_{ij}$
      – *perform the collision between* i *and* j, *and compute* v_i' *and* v_j' *according to the collisional law*
      – *set* $v_i^{n+1} = v_i'$, $v_j^{n+1} = v_j'$
      else
      – *set* $v_i^{n+1} = v_i^n$, $v_j^{n+1} = v_j^n$
  - *set* $v_i^{n+1} = v_i^n$ *for the* $N - 2N_c$ *particles that have not been selected*

end for

Remark 4.1
The terminology 'dummy collision' is here used to denote a fictitious collision between two particles which undergo the acceptance–rejection procedure. Sometimes other authors refer to these kind of collisions as 'trial collision' or 'candidate collision'.

During each step, all the other $N - 2N_c$ particle velocities remain unchanged. Here, by $\mathrm{Iround}(x)$, we denote a suitable integer rounding of a positive real number x. In our algorithm, we choose

$$\mathrm{Iround}(x) = \begin{cases} [x] & \text{with probability } [x] + 1 - x \\ [x] + 1 & \text{with probability } x - [x] \end{cases}$$

where $[x]$ denotes the integer part of x.

The post-collisional velocities are computed through relations

$$v_i' = \frac{v_i + v_j}{2} + \frac{|v_i - v_j|}{2}\,\omega, \quad v_j' = \frac{v_i + v_j}{2} - \frac{|v_i - v_j|}{2}\,\omega \tag{39}$$

where ω is chosen uniformly in the unit sphere, according to

$$\omega = \begin{pmatrix} \cos\phi \sin\theta \\ \sin\phi \sin\theta \\ \cos\theta \end{pmatrix}, \quad \theta = \arccos(2\xi_1 - 1), \quad \phi = 2\pi\xi_2 \tag{40}$$

and ξ_1, ξ_2 are uniformly distributed random variables in $[0,1]$.

The upper bound $\bar{\sigma}$ should be chosen as small as possible, to avoid inefficient rejection, and it should be computed fast.

An upper bound can be derived taking $\bar{\sigma}$ as

$$\bar{\sigma} = \max_{v_i, v_j} \sigma(|v_i - v_j|) \tag{41}$$

However this computation would require $O(N^2)$ operations. Thus it is preferable to use an upper bound of (41) given by

$$\bar{\sigma} = \sigma(2\Delta v), \quad \Delta v = \max_i |v_i - \bar{v}|, \quad \bar{v} = \sum_i v_i/N \tag{42}$$

Remark 4.2

Note that if the time step is small enough, only a small fraction of particles, let us say N_c, will collide. The computational cost of the collisions is therefore $O(N_c)$. On the other hand, the cost of the computation of the upper bound $\bar{\sigma}$ is $O(N)$, which may be much larger than $O(N_c)$. A possible way to overcome this difficulty is to update at each time step the value of the upper bound $\bar{\sigma}$ only if it increases. This may be done as follows. During the computation of the collision between particles i and j, let $\tilde{v}_i$ and $\tilde{v}_j$ denote the new particle velocities. Then the quantity Δv is updated according to

$$\Delta v = \max(\Delta v, |\tilde{v}_i - \bar{v}|, |\tilde{v}_j - \bar{v}|) \tag{43}$$

At the end of the collision loop, the upper bound on the cross-section is computed as

$$\bar{\sigma} = \sigma(2\Delta v)$$

In space non-homogeneous calculations, assuming that there are several collisional time steps during a convection time step, the bound can be computed according to (42) the first time step and then updated as described above.

4.2. First- and second-order TRMC methods

The first-order TRMC algorithm is based on the TR schemes

$$f^{n+1} = A_0 f^n + A_1 f_1 + A_2 M \tag{44}$$

The probabilistic interpretation of the above equation is the following. To sample a particle from f^{n+1}, with probability A_0 we sample the particle from f^n, with probability A_1 we sample the particle from $f_1 = P(f, f)/\mu$ (as in standard DSMC method) and with probability A_2 we sample the particle from a Maxwellian.

In this formulation, the probabilistic interpretation holds uniformly in $\mu\Delta t/\varepsilon$, at variance with standard DSMC, which requires $\mu\Delta t/\varepsilon < 1$. Furthermore, as $\mu\Delta t/\varepsilon \to \infty$, the distribution at time $n+1$ is sampled from a Maxwellian. In this limit, the density f^{n+1} relaxes immediately to its equilibrium distribution. In a space non-homogeneous case, this would be equivalent to a particle method for Euler equations proposed by Pullin [15].

The Monte Carlo schemes described above are conservative in the mean. It is possible to make it exactly conservative by selecting collision pairs uniformly, rather than individual particles, and by using a suitable algorithm for sampling a set of particles with prescribed momentum and energy from a Maxwellian. To this aim one can adopt the original algorithm proposed by Pullin [26]. An alternative and simpler method consists in rescaling the particles sampled from the Maxwellian in order to have exact preservation of the moments.

Suppose that we want to sample N_M particles by a Maxwellian with mean velocity u and energy E. First we have to sample the particles v_i, $i = 1, \ldots, N_M$ from a Gaussian density. To sample two of this particles v_i, v_j we can use the Box–Muller method

$$v_i = u + \sqrt{2T}\rho\cos(\theta_i), \quad v_j = u + \sqrt{2T}\rho\sin(\theta_i)$$

with T given by (8) and

$$\rho = \sqrt{-\log(\xi_1)}, \quad \theta_i = 2\pi\xi_2$$

where ξ_1, ξ_2 are uniformly distributed random variables in $[0, 1]$.

Let now

$$v = \frac{1}{N}\sum_{i=1}^{n} v_i, \quad E' = \frac{1}{2N}\sum_{i=1}^{n} v_i^2$$

be the mean velocity and energy of the sampled particles (we fix for simplicity the mass of a single particle $m = 1$). We want to rescale the samples using a scalar τ and a vector λ such that

$$\frac{1}{N}\sum_{i=1}^{N}\frac{v_i - \lambda}{\tau} = u \tag{45}$$

and

$$\frac{1}{2N}\sum_{i=1}^{N}\frac{(v_i - \lambda)^2}{\tau^2} = E \tag{46}$$

Solving the system we obtain

$$\tau^2 = \left(E' - \frac{v^2}{2}\right)\Big/\left(E - \frac{u^2}{2}\right) \tag{47}$$

and

$$\lambda = v - \tau u \tag{48}$$

Note that the right-hand side of Equation (47) is non negative and thus the system admits always a solution.

Remark 4.3
Since the v_i are normally distributed and the transformation $v_i' = (v_i - \lambda)/\tau$ is linear, the rescaled velocities v_i' remain normally distributed.

The conservative version of the methods can be formalized in the following algorithm.

Algorithm 4.2 (*first-order TRMC for VHS molecules*)

- *compute the initial velocity of the particles*, $\{v_i^0,\ i = 1,\ldots,N\}$, *by sampling them from the initial density* $f_0(v)$
- for $n = 1$ to n_{TOT}
  given $\{v_i^n,\ i = 1,\ldots,N\}$,
  - *compute an upper bound* $\bar{\sigma}$ *of the cross-section*
  - *set* $\tau = 1 - \exp(-\rho\bar{\sigma}\Delta t/\varepsilon)$
  - *compute* $A_1(\tau)$, $A_2(\tau)$
  - *set* $N_c = \text{Iround}(NA_1/2)$
  - *perform* N_c *dummy collisions, as in Algorithm* 4.1
  - *set* $N_M = \text{Iround}(NA_2)$
  - *select* N_M *particles among those that have not collided, and compute their mean momentum and energy*
  - *sample* N_M *particles from the Maxwellian with the above momentum and energy, and replace the* N_M *selected particles with the sampled ones*
  - *set* $v_i^{n+1} = v_i^n$ *for all the* $N - 2N_c - N_M$ *particles that have not been selected*

end for

A second-order Monte Carlo scheme is obtained by the TR scheme

$$f^{n+1} = A_0 f^n + A_1 f_1 + A_2 f_2 + A_3 M \tag{49}$$

with

$$f_1 = \frac{P(f^n, f^n)}{\mu}, \quad f_2 = \frac{P(f^n, f_1)}{\mu}$$

Given N particles distributed according to f^n, the probabilistic interpretation of scheme 49 is the following: NA_0 particles will not collide; NA_1 will be sampled from f_1 (as in the first-order scheme); NA_2 will be sampled from f_2; i.e. $NA_2/2$ particles sampled from f^n will undergo dummy collisions with $NA_2/2$ particles sampled from f_1; and NA_3 particles will be sampled from a Maxwellian.

Once again, the methods can be made conservative using the same techniques adopted in the first-order scheme. The various steps of the method can be summarized in the following algorithm.

Algorithm 4.3 (*second-order TRMC for VHS molecules*)

- *compute the initial velocity of the particles*, $\{v_i^0,\ i=1,\dots,N\}$, *by sampling them from the initial density* $f_0(v)$
- for $n=1$ to n_{TOT}
  given $\{v_i^n,\ i=1,\dots,N\}$,
  - *compute an upper bound* $\bar{\sigma}$ *of the cross-section*
  - *set* $\tau = 1-\exp(-\rho\bar{\sigma}\Delta t/\varepsilon)$
  - *compute* $A_1(\tau)$, $A_2(\tau)$, $A_3(\tau)$
  - *set* $N_1 = \mathrm{Iround}(NA_1/2)$, $N_2 = \mathrm{Iround}(NA_2/4)$
  - *select* N_1+N_2 *dummy collision pairs* (i,j) *uniformly among all possible pairs*
  - *for* N_1 *pairs*
    - *compute the relative cross-section* $\sigma_{ij}=\sigma(|v_i-v_j|)$
    - if $\bar{\sigma}\,\mathrm{Rand} < \sigma_{ij}$
      - *perform the collision between* i *and* j, *and compute* v_i' *and* v_j' *according to the collisional law*
      - *set* $v_i^{n+1}=v_i'$, $v_j^{n+1}=v_j'$
  - *for* N_2 *pairs*
    - *compute the relative cross-section* $\sigma_{ij}=\sigma(|v_i-v_j|)$
    - if $\bar{\sigma}\,\mathrm{Rand} < \sigma_{ij}$
      - *perform the collision between* i *and* j, *compute* v_i' *and* v_j' *according to the collisional law and store them*
  - *select* $2N_2$ *particles from* f^n
  - *perform the collision of these selected particles with the second set of* $2N_2$ *particles that have collided once*
  - *update the velocity of the* $4N_2$ *particles with the outcome of the* $2N_2$ *collisions* (*of particles that have never collided before with particles that collided once*)
  - *set* $N_M = \mathrm{Iround}(NA_3)$
  - *replace* N_M *particles with samples from Maxwellian, as in Algorithm* 4.2
  - *set* $v_i^{n+1}=v_i^n$ *for all the* $N-2N_1-4N_2-N_M$ *particles that have not been selected*

end for

Similarly, higher order TRMC methods can be constructed. For example, a third-order scheme is obtained from

$$f^{n+1} = A_0 f^n + A_1 f_1 + A_2 f_2 + A_3 f_3 + A_4 M \tag{50}$$

with

$$f_1 = \frac{P(f^n, f^n)}{\mu}, \quad f_2 = \frac{P(f^n, f_1)}{\mu}, \quad f_3 = \frac{1}{3\mu}[2P(f^n, f_2) + P(f_1, f_1)]$$

We omit for brevity the details of the resulting Monte Carlo algorithm. We remark here that the TR scheme is a direct consequence of the time discretization of the Boltzmann equation. In this respect, the choice of a particular Monte Carlo scheme used to model the collision is not crucial. Here we considered a commonly used Monte Carlo scheme. If a different technique is used to model the collision, then the same technique could be used in conjunction with the TR discretization.

5. NUMERICAL RESULTS

In this section we compare DSMC and TRMC methods on a two-dimensional space non homogeneous test problem. We will refer to first- and second-order TRMC methods as TRMC I and TRMC II, respectively.

The physical problem we will study is represented by a rarefied gas flow around an elliptical section of an object. The rectangular domain Ω has been divided into a regular grid of cells. If we assume that in each cell the density is constant during the collision step, we can apply the algorithms previously seen. This is physically equivalent to say that each particle can collide only with particles of the same cell.

5.1. Free transport

In a spatial homogeneous case we supposed that the density function to be a probability function, that is with unitary mass. In spatially non-homogeneous cases the integral in the velocity determines the gas density number

$$\int_{\mathbb{R}^3} f(x,v,t)\,\mathrm{d}v = \frac{\rho}{m} \tag{51}$$

where m is a gas molecule mass. The algorithms seen in the previous sections can be modified considering

$$\mu = 4\pi\bar{\sigma}\rho/m \tag{52}$$

The density ρ is proportional to the number of particles in each cell j

$$\rho_j = N_j m^* \tag{53}$$

where m^* is the mass of the particles used in the simulation.

The transport step is made easily applying to each particle i

$$x_i' = x_i + v_i \Delta t \tag{54}$$

5.2. Particle–surface interaction

At the surface of the obstacle the particles are absorbed and remitted in according with the Maxwellian distribution of a gas at the same temperature of the object.

To compute the new ingoing velocity we must sample an ingoing particle from the flux corresponding to a Maxwellian with zero mean velocity and at the temperature of the wall. We describe here the method we used in the case of a two-dimensional elliptic object.

Let Δt^* be the time of free flow of the particle before colliding the object (which can be computed analytically for simple geometries such as the case of circular or elliptical objects, or using a suitable numerical method for more general geometries). The contact point particle-object will then be

$$x_i^* = x_i + v_i \Delta t^*$$

There are several ways to calculate the new position and velocity of a particle after a collision with the boundary. For example, if $v_M = (v_M^x, v_M^y, v_M^z)$ is the velocity sampled by the Maxwellian flux corresponding to the thermal equilibrium gas-obstacle and $\{k, n, t\}$ is the orthogonal set of unitary vectors that characterize, respectively, the z-axis, the normal and the tangent to the surface at the contact point, then the new outgoing velocity of the particle will be

$$v_i' = |v_M^x| n + v_M^y t + v_M^z k \tag{55}$$

and its position will be determined by

$$x_i' = x_i^* + v_i'(\Delta t - \Delta t^*) \tag{56}$$

where x_i^* is the contact point and Δt is the time step.

5.3. *Two-dimensional flow past an ellipse*

In our calculations, the upstream state is characterized by a Mach number M with

$$\rho = 1.0, \quad T = 5.0, \quad T_{\text{obj}} = 10.0$$

where T and T_{obj} are, respectively, the gas and the object temperature. The upstream mean velocity is then given by

$$u_x = -M\sqrt{(\gamma T)}, \quad u_y = 0, \quad u_z = 0$$

with $\gamma = \frac{5}{3}$ since we have considered a three-dimensional monatomic gas in velocity space.

The infinite physical space is truncated to the finite region $[0, 1.5] \times [0, 1.2]$. We report the results obtained with the different schemes using 75×60 space cells and 30 particles ingoing in each downstream cell.

Since we are computing a stationary solution after a fixed initial time, we can strongly improve the accuracy of the Monte Carlo solution by averaging in time the solution itself. In all our simulations we report the results obtained after averaging the solution over 400 time steps after a sufficiently large computational time has been reached. As a reference solution to estimate the relative L_2-error norms we used 50 particles per cell and 2000 averages with DSMC.

The collisional time step in DSMC has been computed adaptively cell by cell to satisfy the stability condition. At variance in TRMC the collisional time step has been taken $C\Delta t$, where $C \leqslant 1$ is a constant and Δt is the free flow time step. In the graphs reporting the number of collisions in time we have considered the sampling from a Maxwellian in TRMC like a collision. We refer to Reference [27] for similar results on DSMC computations of flows past an ellipse.

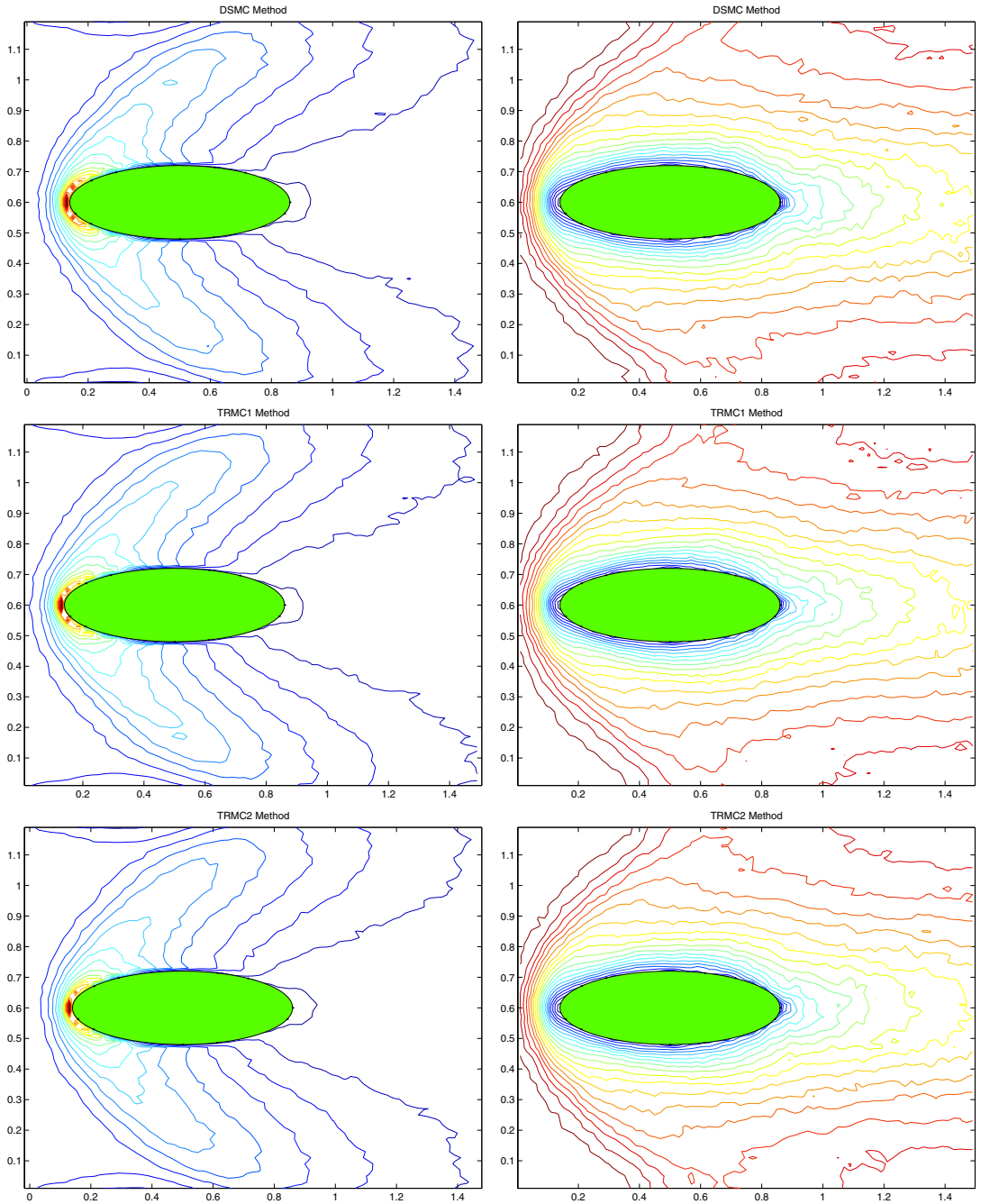

Figure 1. Iso-values of the density ρ (left) and mean velocity u (right) for $\varepsilon = 0.1$ and $M = 5$; DSMC (top), TRMC I (middle), TRMC II (bottom).

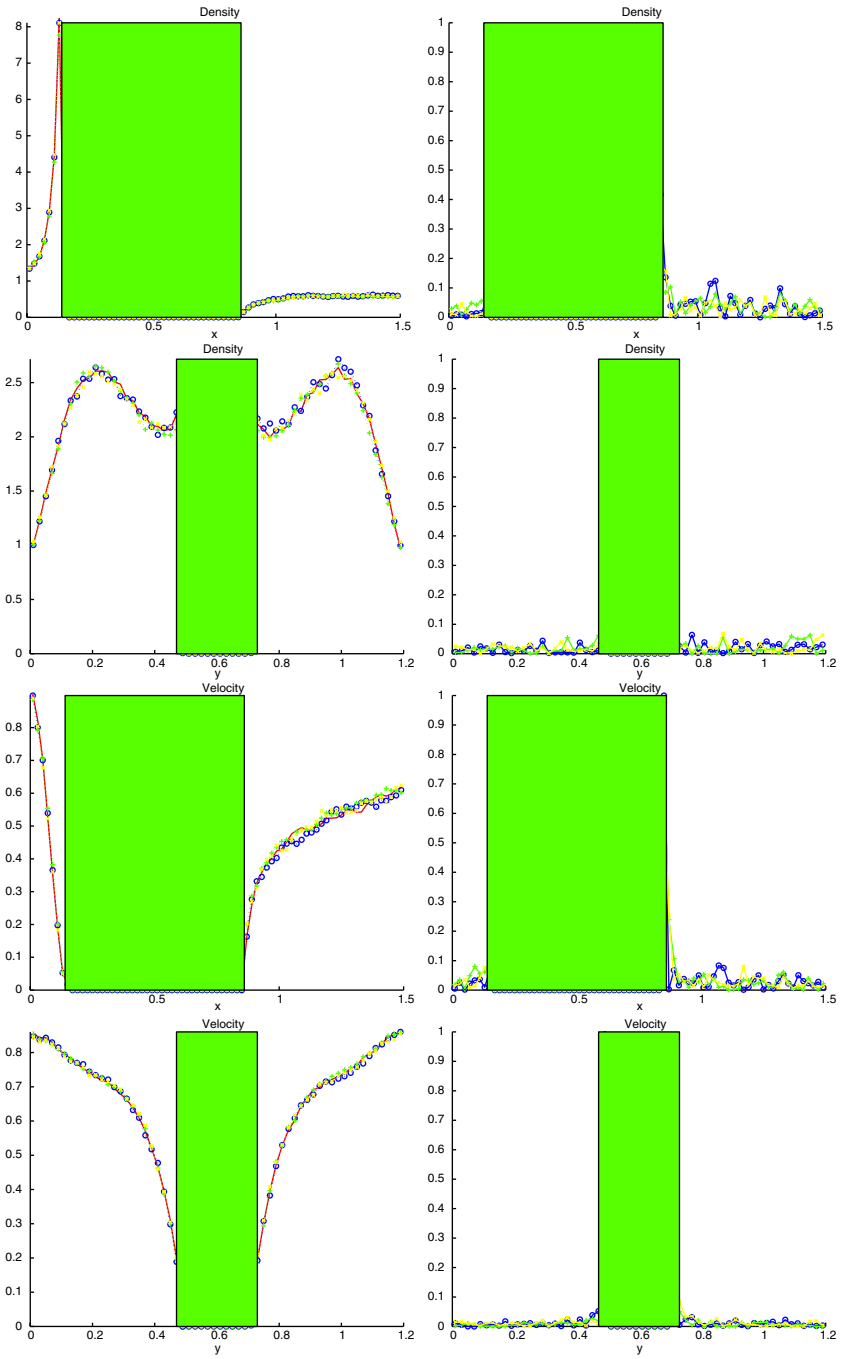

Figure 2. Longitudinal and transversal sections of density and velocity (left) and relative errors (right) at $y = 6$ and $x = 5$, respectively, for $\varepsilon = 0.1$ and $M = 5$; DSMC ($\circ$), TRMC I ($+$), TRMC II ($\times$).

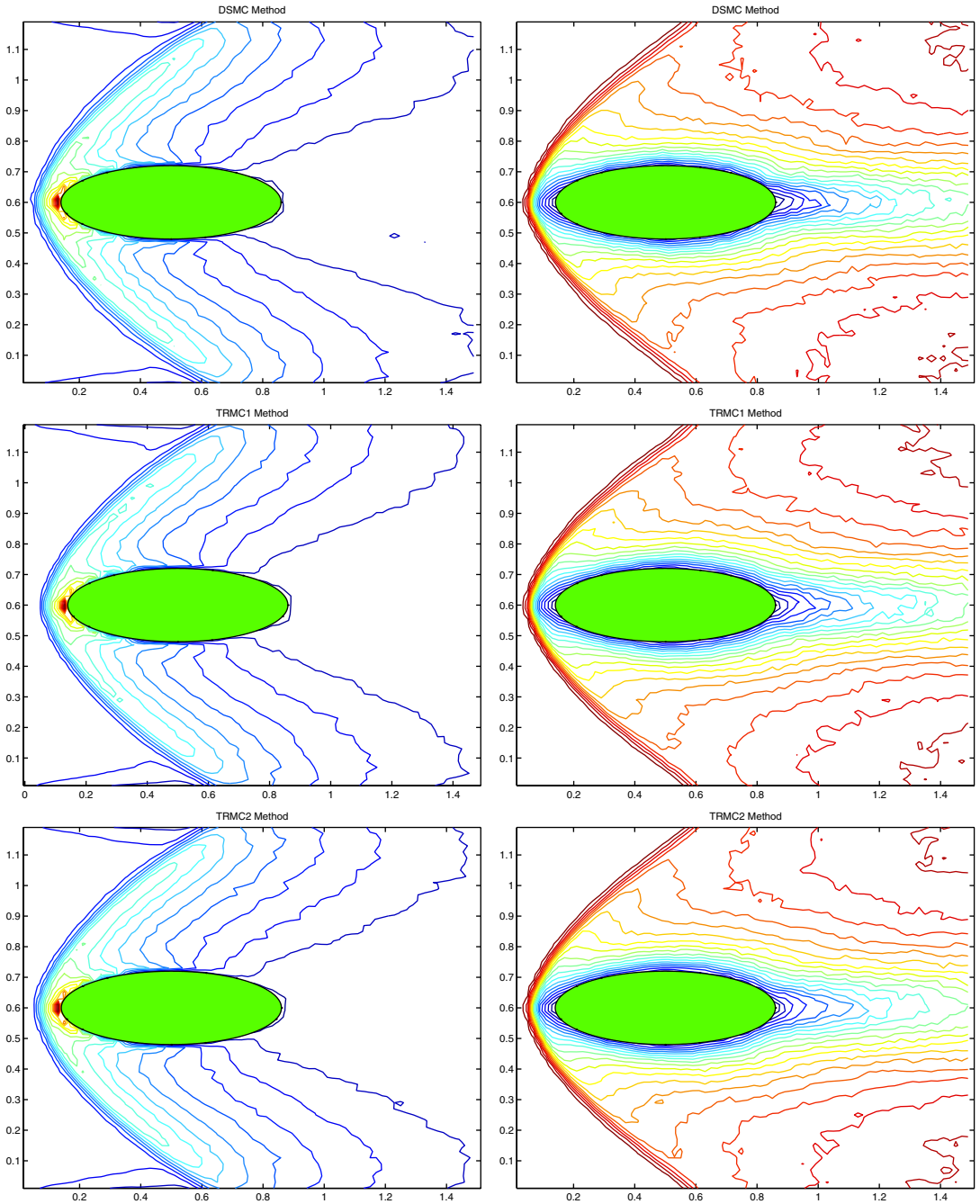

Figure 3. Iso-values of the density ρ (left) and mean velocity u (right) for $\varepsilon = 0.01$ and $M = 5$; DSMC(top), TRMC I (middle), TRMC II (bottom).

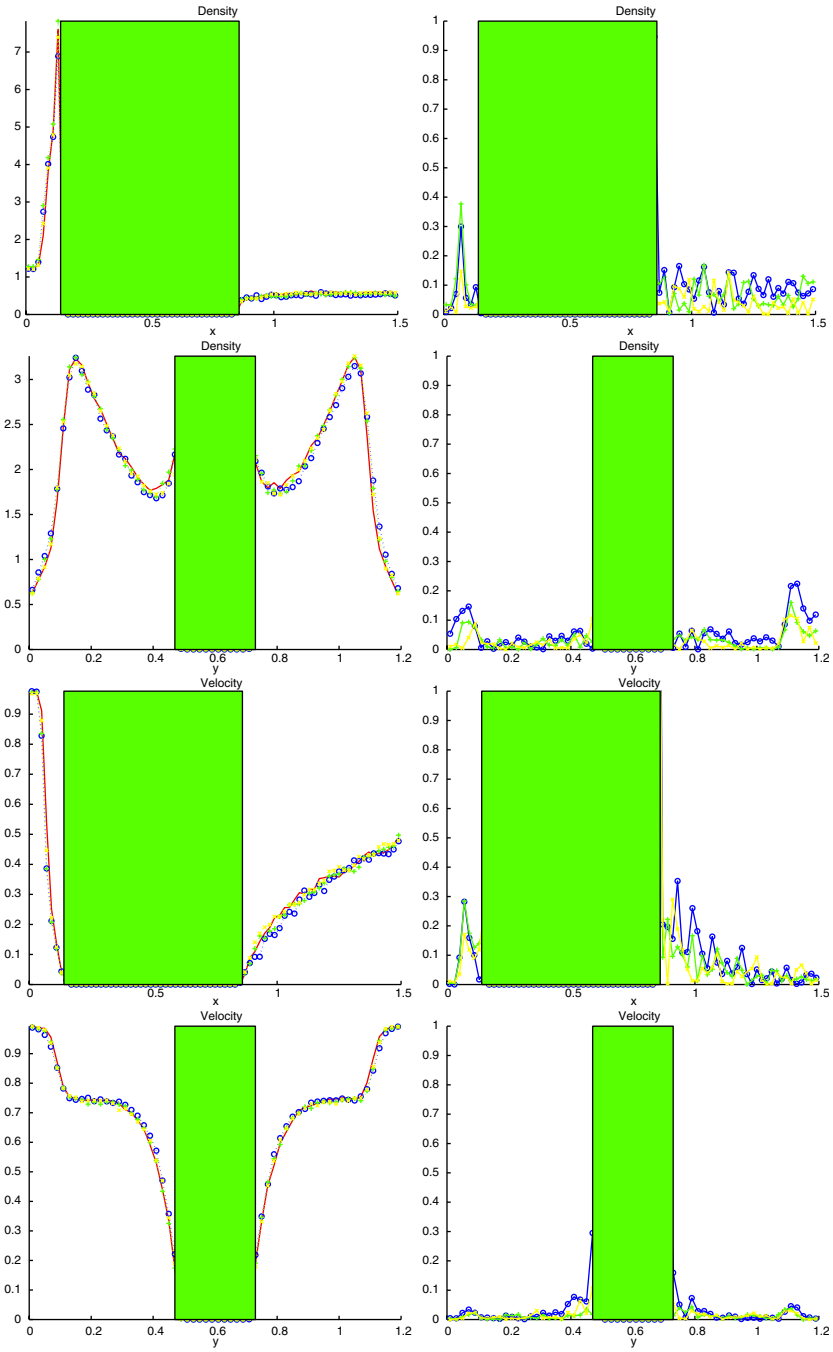

Figure 4. Longitudinal and transversal sections of density and velocity (left) and relative errors (right) at $y = 6$ and $x = 5$, respectively, for $\varepsilon = 0.01$ and $M = 5$; DSMC ($\circ$), TRMC I ($+$), TRMC II ($\times$).

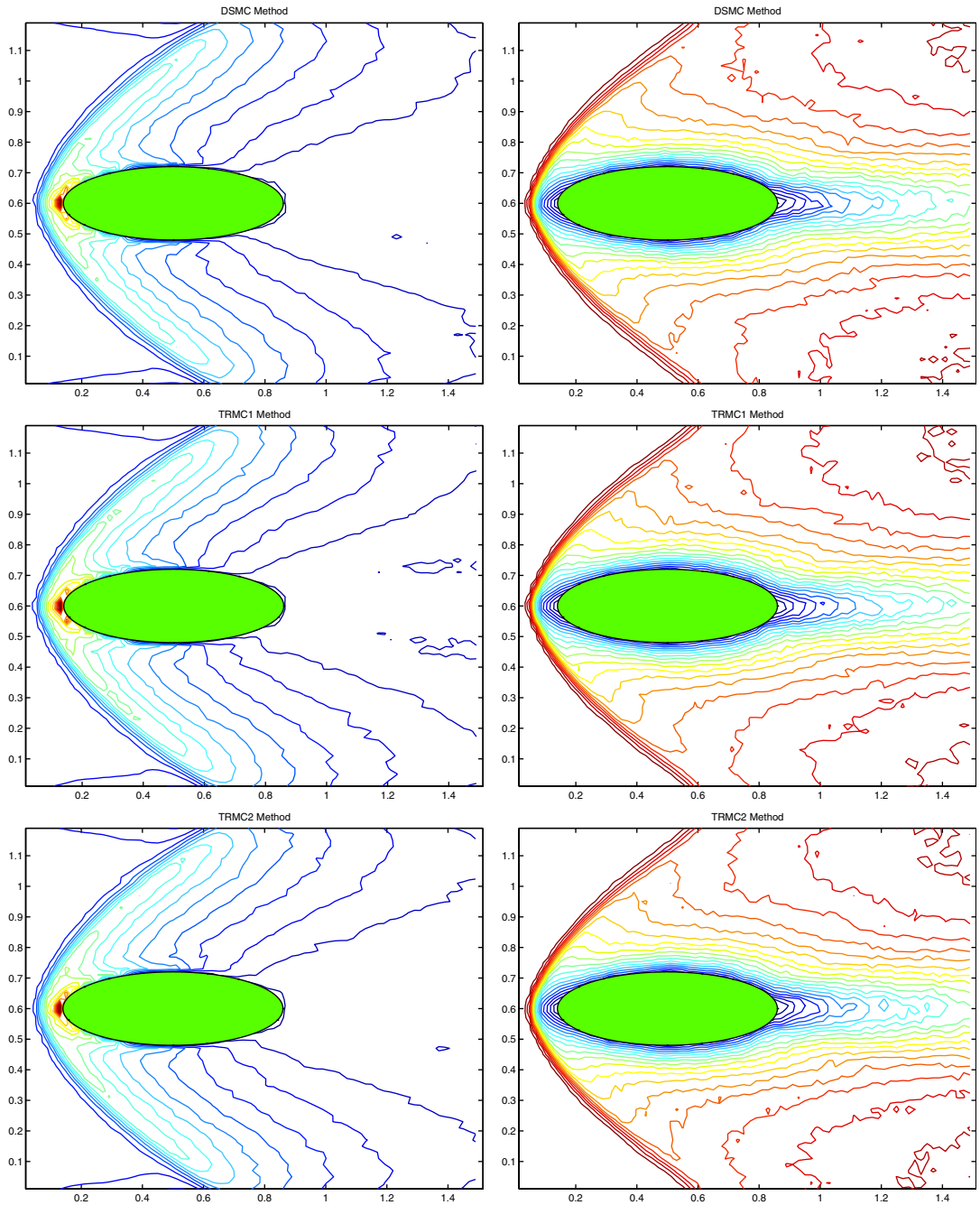

Figure 5. Iso-values of the density ρ (left) and mean velocity u (right) for $\varepsilon = 0.001$ and $M = 5$; DSMC (top), TRMC I (middle), TRMC II (bottom).

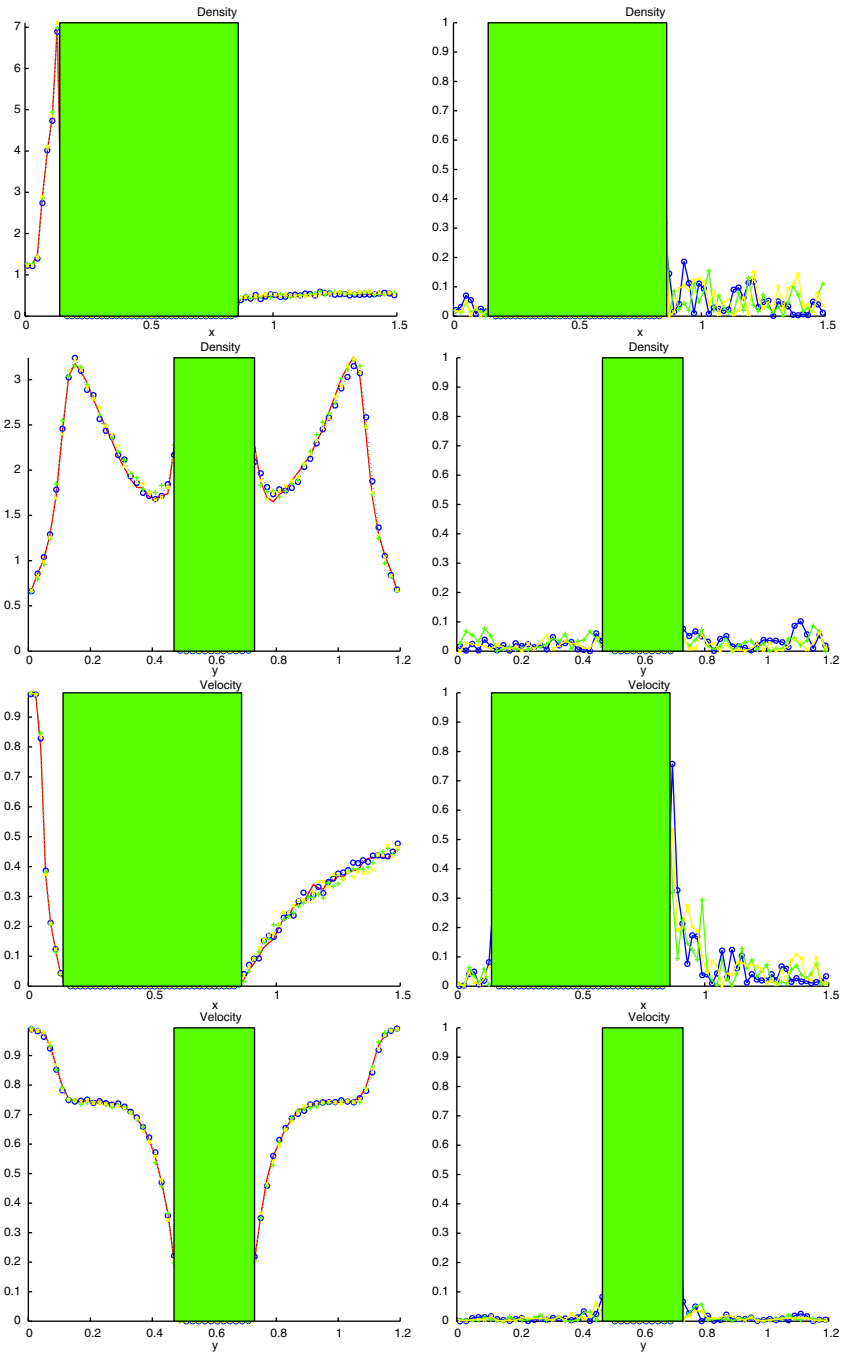

Figure 6. Longitudinal and transversal sections of density and velocity (left) and relative errors (right) at $y = 6$ and $x = 5$, respectively, for $\varepsilon = 0.001$ and $M = 5$; DSMC ($\circ$), TRMC I ($+$), TRMC II ($\times$).

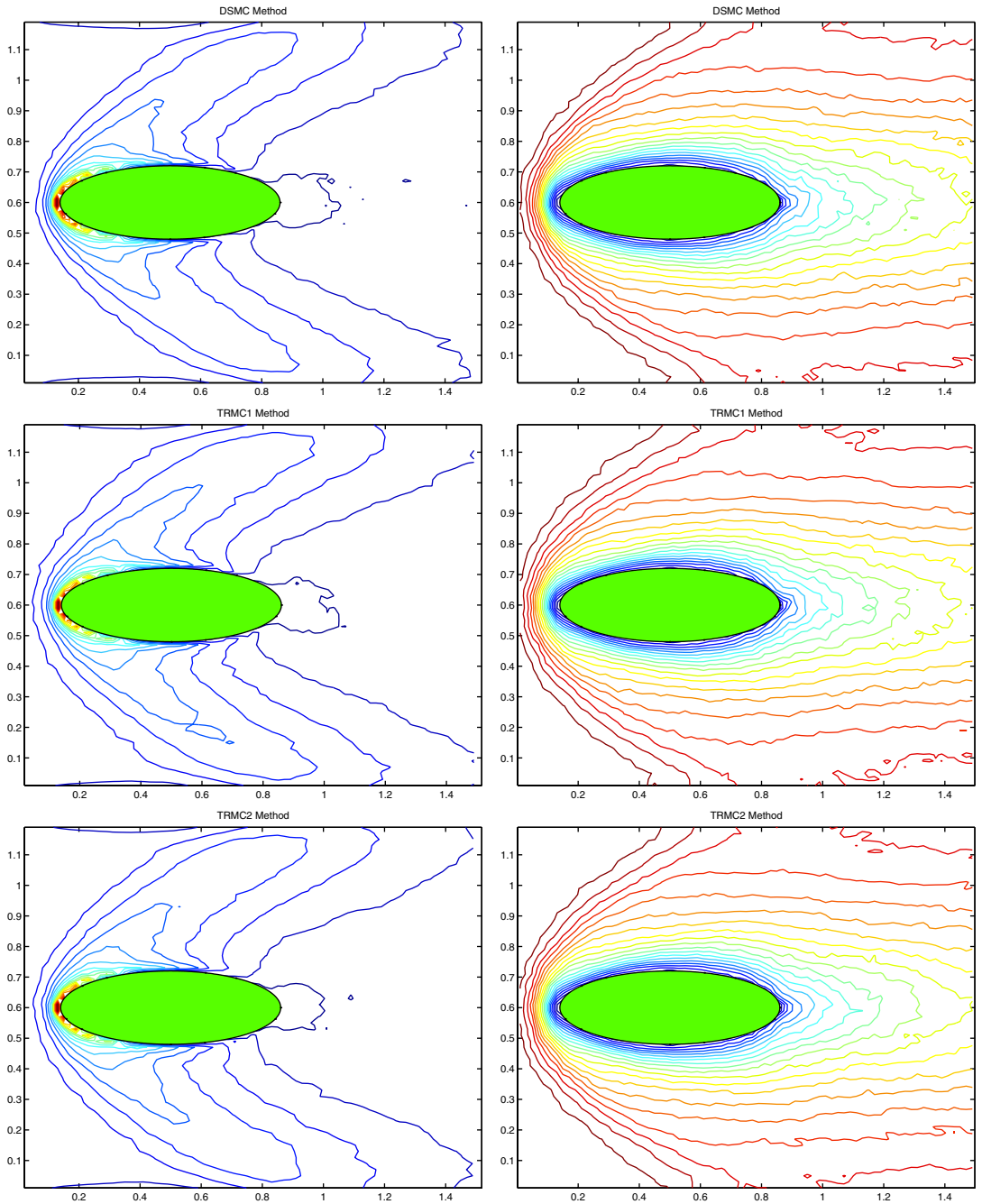

Figure 7. Iso-values of the density ρ (left) and mean velocity u (right) for $\varepsilon = 0.1$ and $M = 10$; DSMC (top), TRMC I (middle), TRMC II (bottom).

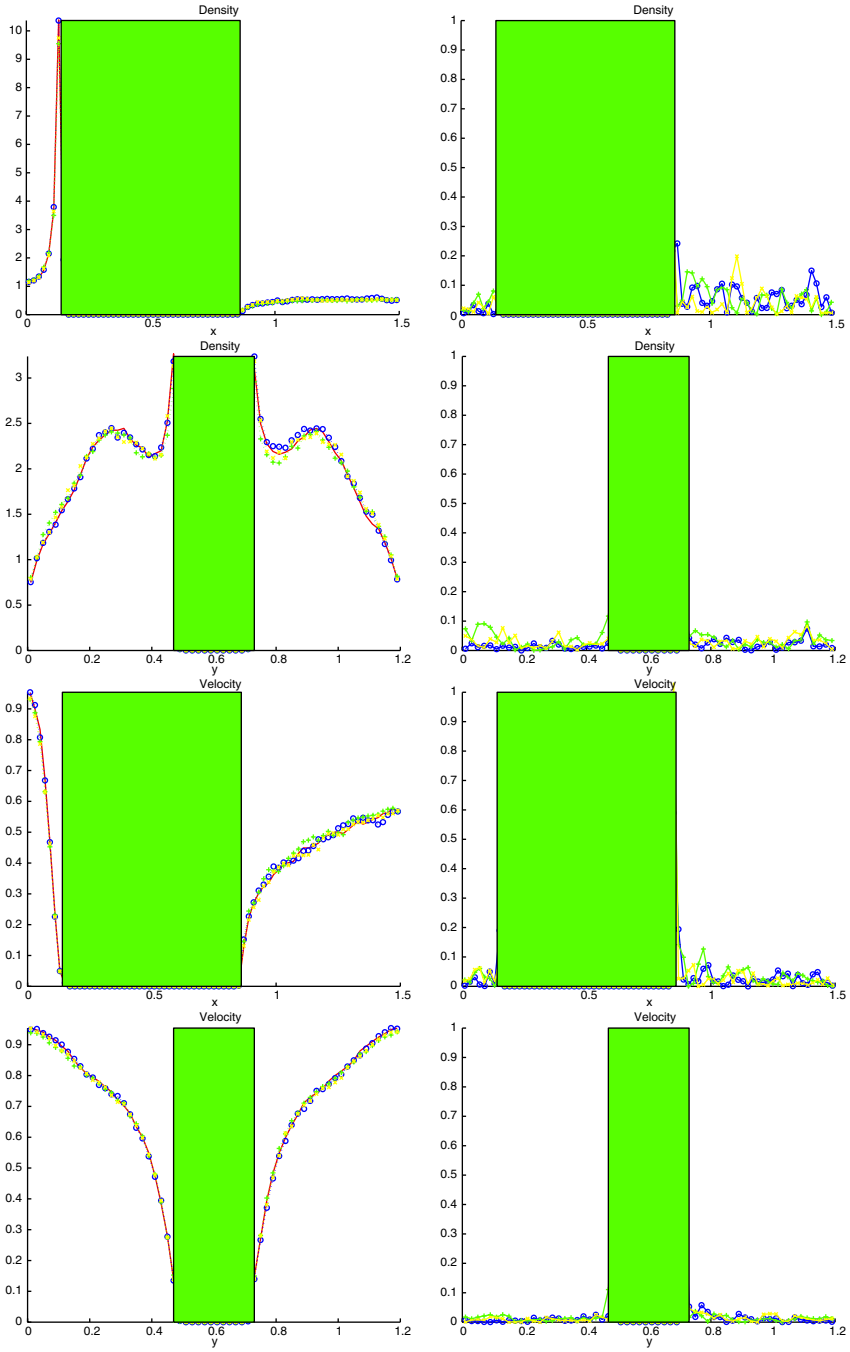

Figure 8. Longitudinal and transversal sections of density and velocity (left) and relative errors (right) at $y = 6$ and $x = 5$, respectively, for $\varepsilon = 0.1$ and $M = 10$; DSMC ($\circ$), TRMC I ($+$), TRMC II ($\times$).

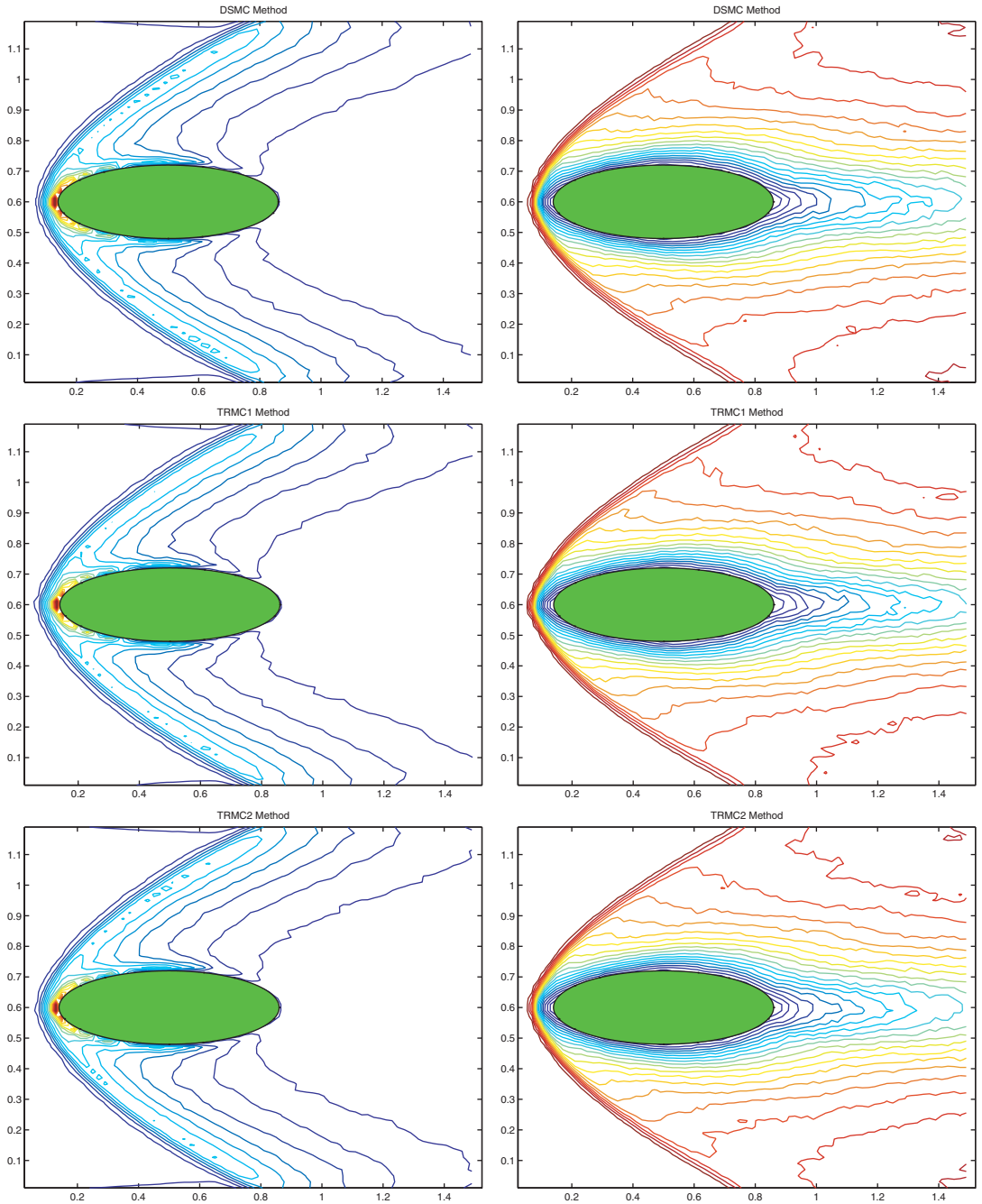

Figure 9. Iso-values of the density ρ (left) and mean velocity u (right) for $\varepsilon = 0.01$ and $M = 10$; DSMC (top), TRMC I (middle), TRMC II (bottom).

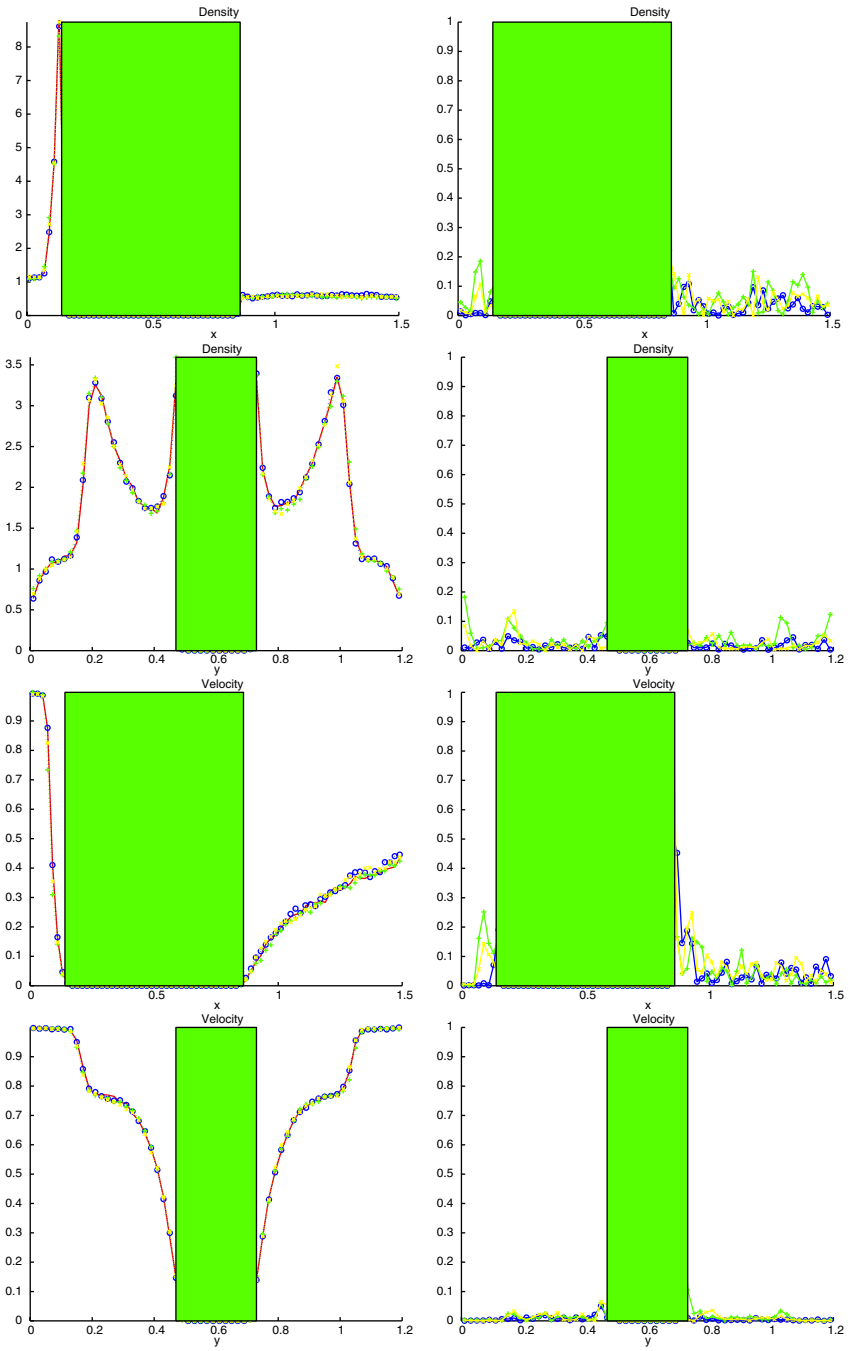

Figure 10. Longitudinal and transversal sections of density and velocity (left) and relative errors (right) at $y = 6$ and $x = 5$, respectively, for $\varepsilon = 0.01$ and $M = 10$; DSMC ($\circ$), TRMC I ($+$), TRMC II ($\times$).

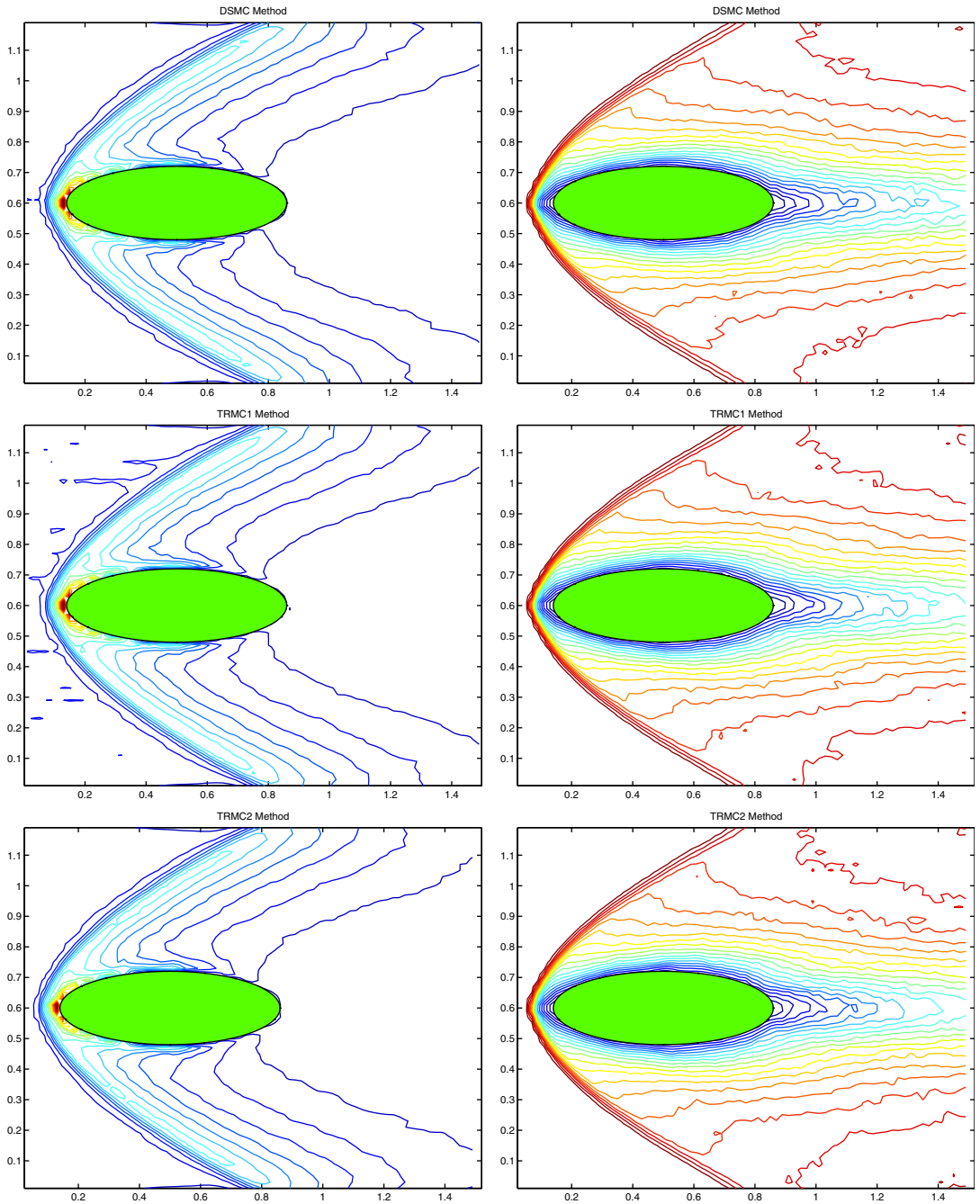

Figure 11. Iso-values of the density ρ (left) and mean velocity u (right) for $\varepsilon = 0.001$ and $M = 10$; DSMC (top), TRMC I (middle), TRMC II (bottom).

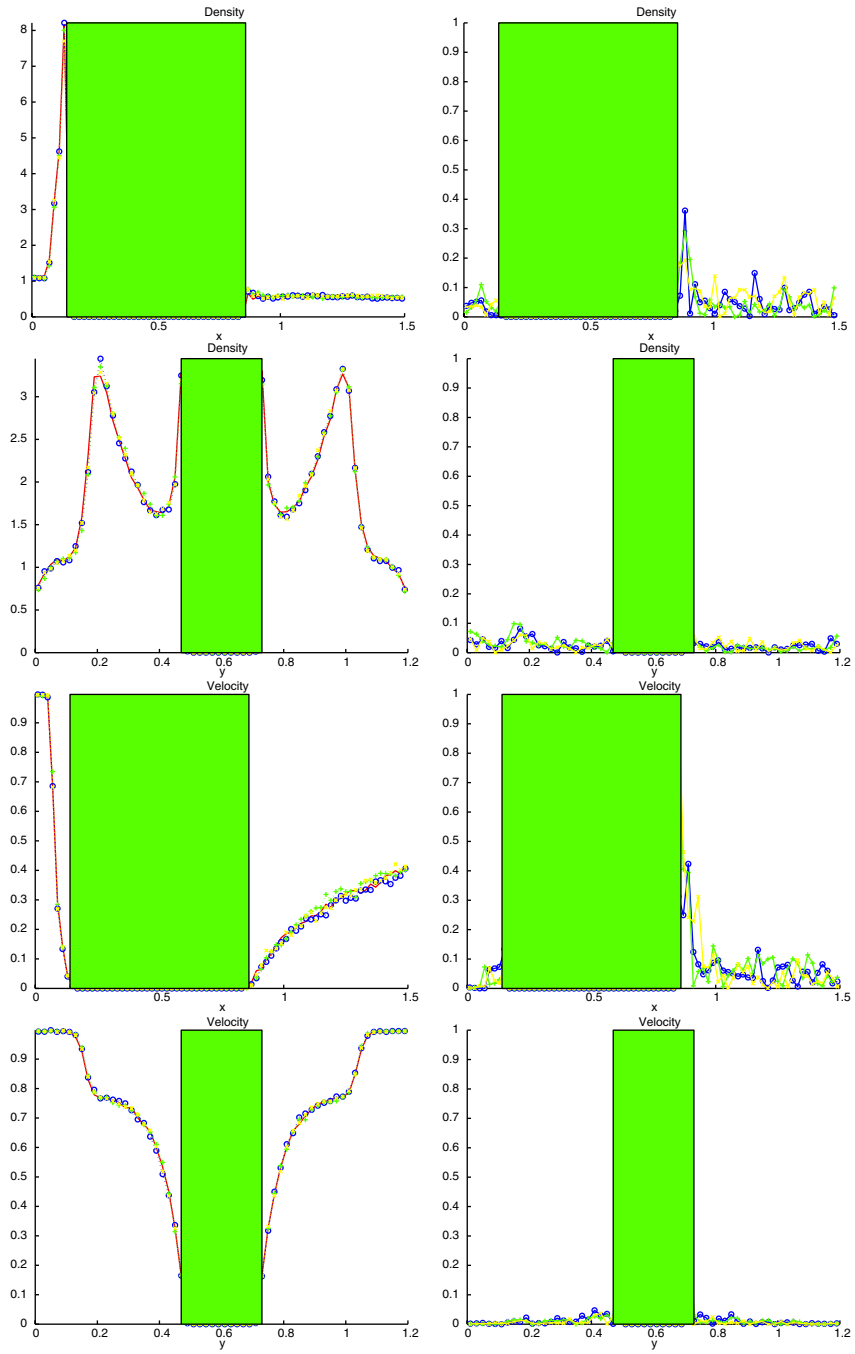

Figure 12. Longitudinal and transversal sections of density and velocity (left) and relative errors (right) at $y = 6$ and $x = 5$, respectively, for $\varepsilon = 0.01$ and $M = 10$; DSMC ($\circ$), TRMC I ($+$), TRMC II ($\times$).

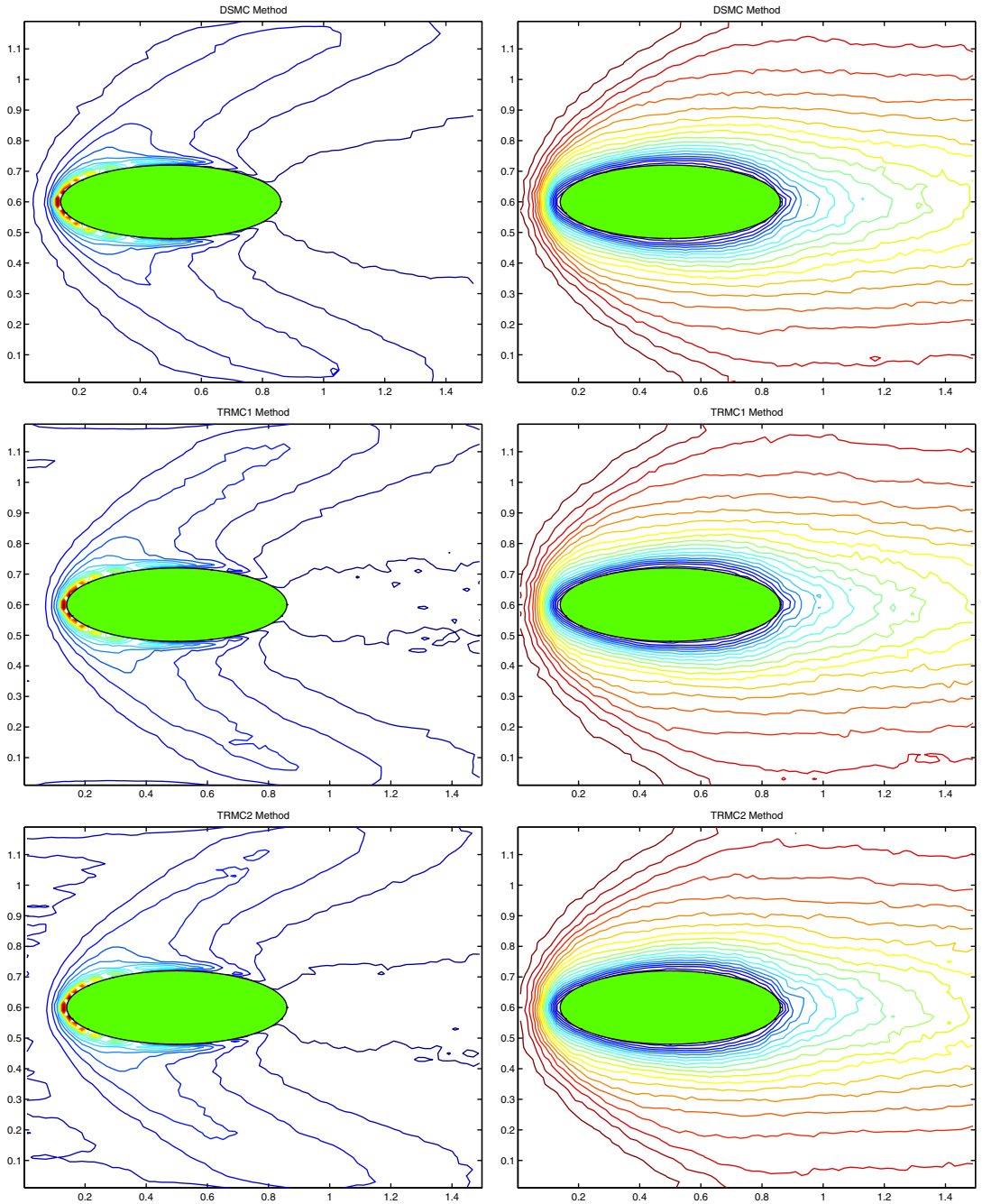

Figure 13. Iso-values of the density ρ (left) and mean velocity u (right) for $\varepsilon = 0.1$ and $M = 20$; DSMC (top), TRMC I (middle), TRMC II (bottom).

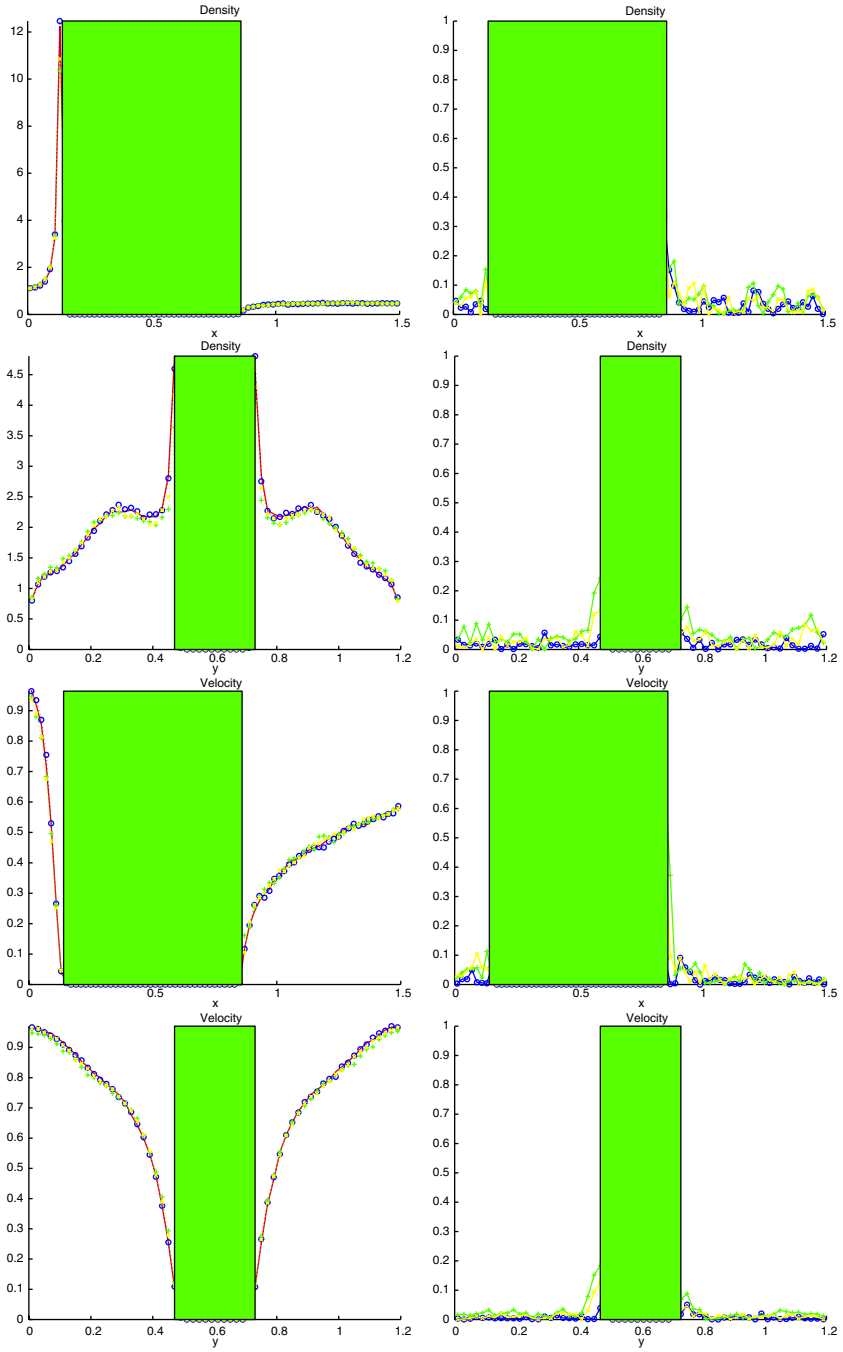

Figure 14. Longitudinal and transversal sections of density and velocity (left) and relative errors (right) at $y = 6$ and $x = 5$, respectively, for $\varepsilon = 0.1$ and $M = 20$; DSMC ($\circ$), TRMC I ($+$), TRMC II ($\times$).

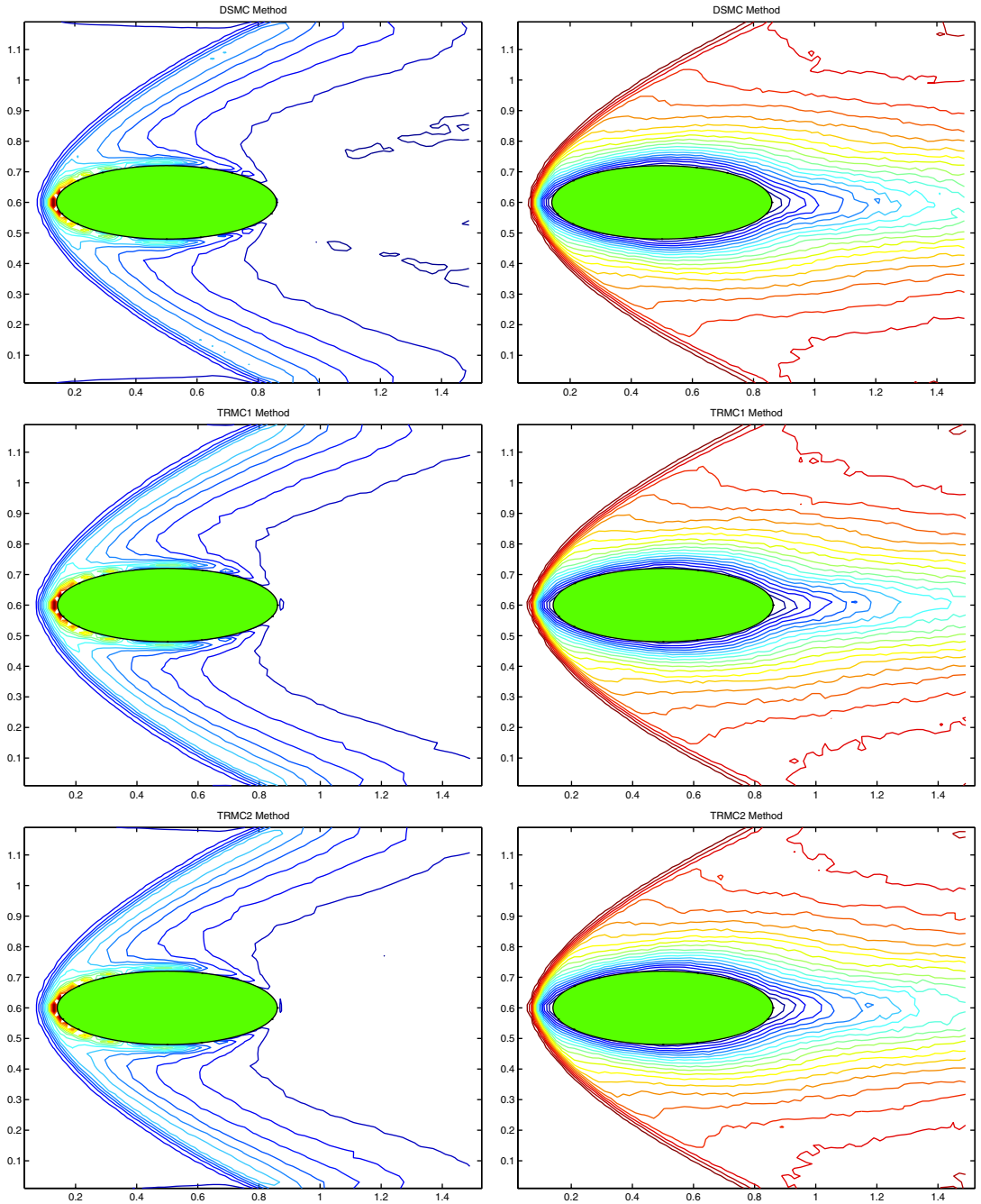

Figure 15. Iso-values of the density ρ (left) and mean velocity u (right) for $\varepsilon = 0.01$ and $M = 20$; DSMC (top), TRMC I (middle), TRMC II (bottom).

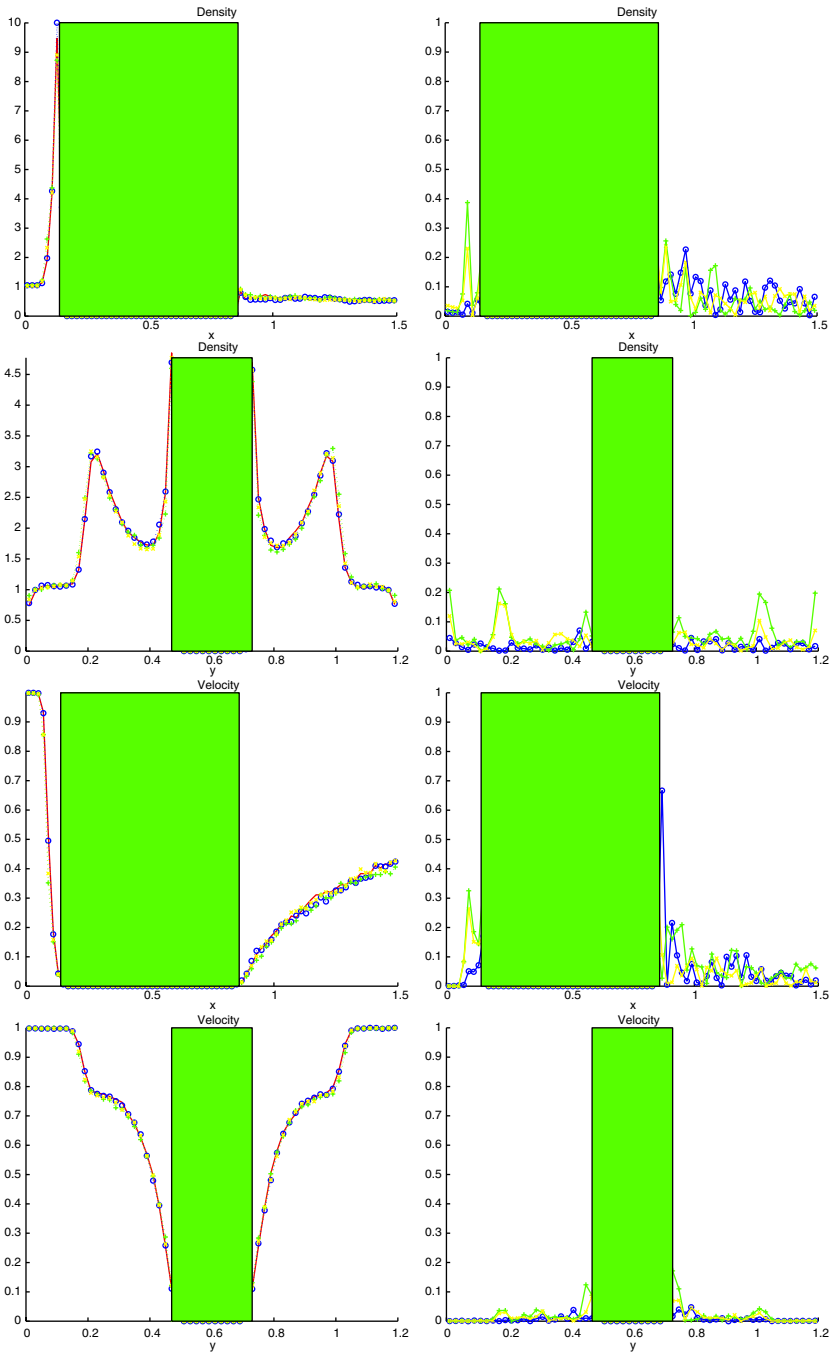

Figure 16. Longitudinal and transversal sections of density and velocity (left) and relative errors (right) at $y = 6$ and $x = 5$, respectively, for $\varepsilon = 0.01$ and $M = 20$; DSMC ($\circ$), TRMC I ($+$), TRMC II ($\times$).

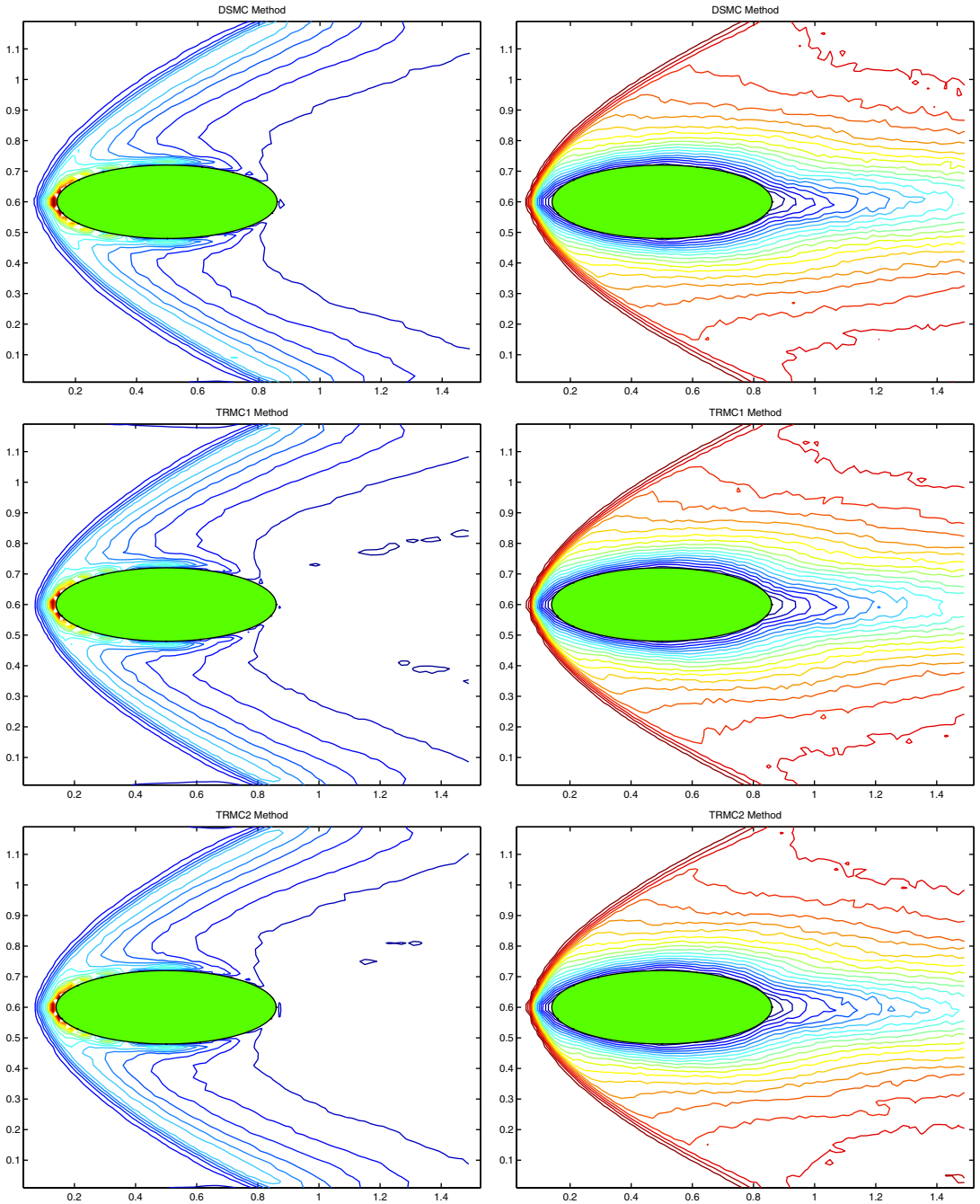

Figure 17. Iso-values of the density ρ (left) and mean velocity u (right) for $\varepsilon = 0.001$ and $M = 20$; DSMC (top), TRMC I (middle), TRMC II (bottom).

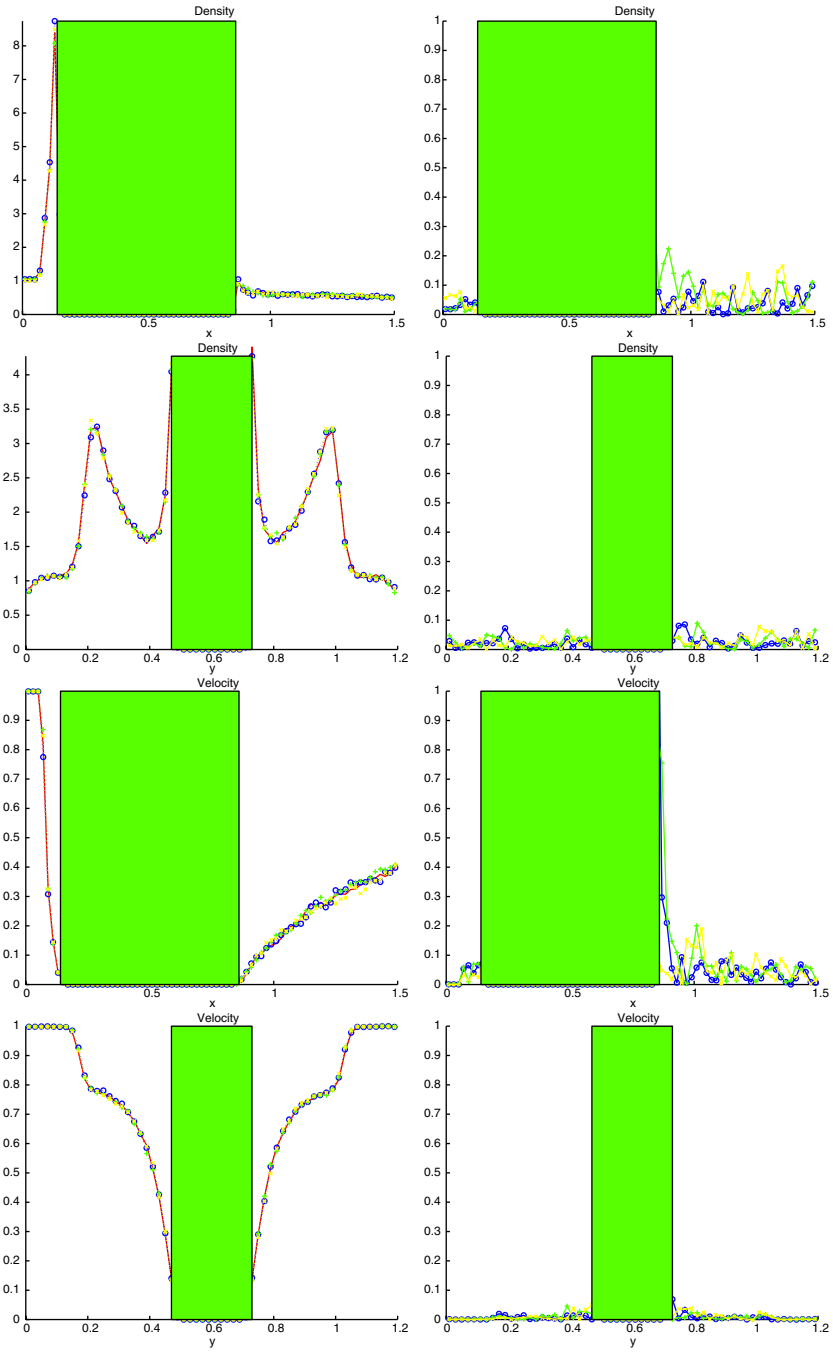

Figure 18. Longitudinal and transversal sections of density and velocity (left) and relative errors (right) at $y = 6$ and $x = 5$, respectively, for $\varepsilon = 0.001$ and $M = 20$; DSMC ($\circ$), TRMC I ($+$), TRMC II ($\times$).

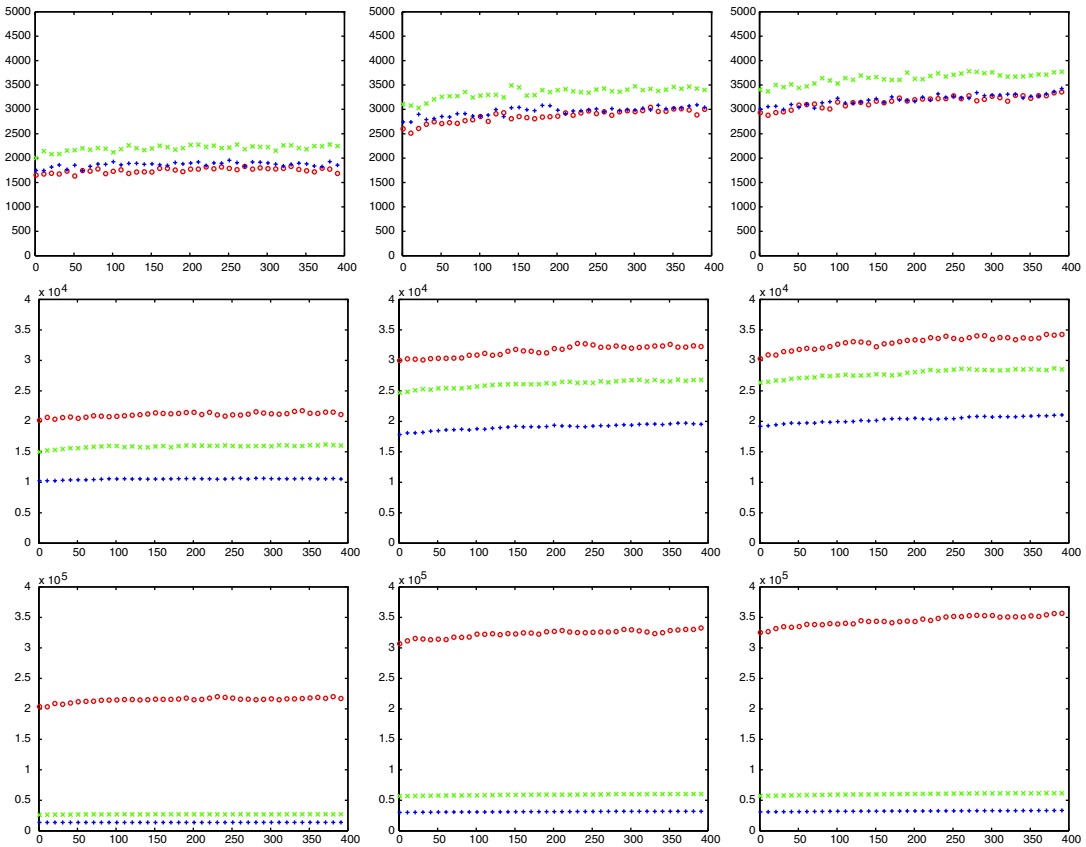

Figure 19. Number of 'collisions' in time, respectively, for $M=1$ (left), $M=10$ (centre), $M=20$ (right). From top to bottom $\varepsilon=0.1, 0.01, 0.001$; DSMC ($\circ$), TRMC I ($+$), TRMC II ($\times$).

We studied the dynamic of the gas for different ranges of the Knudsen number and different values of the Mach number. The isovalues of the density and mean velocity for each test case has been reported. For each value of the Mach number ranging from $5, 10, 20$ the first example shows the case of a very rarefied gas (i.e. $\varepsilon=0.1$) the second the intermediate regime (i.e. $\varepsilon=0.01$) and the last closer to the fluid regime (i.e. $\varepsilon=0.001$) (Figures 1–19).

In the rarefied regime we cannot expect any computational gain of TRMC with respect to DSMC. The numerical results obtained for $C=1$ in TRMC with the different schemes are very similar as well as the efficiency (see Figure 12 left). As expected the sections along the lines $x=5$ and $y=y$ emphasize the higher accuracy obtained with TRMC II (see Figures 2, 4, 6).

For the intermediate regime we have considered the solutions obtained by TRMC with a collisional time of one third of the free flow time ($C=1/3$). Again the solutions are comparable, with an improvement obtained by TRMC II, but with a better computational efficiency in TRMC methods (TRMC I is almost two times faster then DSMC, see Figure 12 centre). The plots of the sections (see Figures 8, 10, 14).

Finally, the last example is near the fluid regime. The improvement of TRMC with $C = 1/5$ over DSMC is clearly evident. The same degree of accuracy is reached with a speed up of computing time of approximatively 10 times for TRMC I and approximatively 5 times for TRMC II.

For lower values of ε the DSMC method becomes unusable due to the increasing number of collisions, while the computational cost of TRMC reaches a constant value which depends only from the number of particles used in the simulation.

6. CONCLUSION

We have presented a Monte Carlo method which is suitable for the numerical simulation of the Boltzmann equation close to fluid regimes. In such fluid limit the methods become a kinetic particle scheme for the Euler equations and result in a greater efficiency if compared to standard DSMC schemes. The methods presented in this paper have limited accuracy in time and for such reason have been compared to Nambu version of DSMC. A recursive TRMC method that does not contain time discretization error is currently under development [9]. Numerical comparison of this last method with Bird's DSMC algorithm will be presented elsewhere.

ACKNOWLEDGEMENTS

We would like to thank Giovanni Russo for the many stimulating discussions and suggestions. The support by the European network HYKE, funded by the EC as contract HPRN-CT-2002-00282, is gratefully acknowledged.

REFERENCES

1. Cercignani C. *The Boltzmann Equation and its Applications*. Springer: New York, 1988.
2. Pareschi L, Russo G. Time relaxed Monte Carlo methods for the Boltzmann equation. *SIAM Journal on Scientific Computing* 2001; **23**:1253–1273.
3. Nanbu K. Direct simulation scheme derived from the Boltzmann equation. *Journal of the Physical Society of Japan* 1980; **49**:2042–2049.
4. Babovsky H. On a simulation scheme for the Boltzmann equation. *Mathematical Methods in the Applied Sciences* 1986; **8**:223–233.
5. Bird GA. *Molecular Gas Dynamics*. Oxford University Press: London, 1976.
6. Babovsky H, Illner R. A convergence proof for Nanbu's simulation method for the full Boltzmann equation. *SIAM Journal on Numerical Analysis* 1989; **26**:45–65.
7. Wagner W. A convergence proof for Bird's direct simulation Monte Carlo method for the Boltzmann equation. *Journal of Statistical Physics* 1992; **66**:1011–1044.
8. Pareschi L, Wennberg B. A recursive Monte Carlo method for the Boltzmann equation in the Maxwellian case. *Monte Carlo Methods and Applications* 2001; **7**:349–358.
9. Pareschi L, Trazzi S, Wennberg B. Recursive time relaxed Monte Carlo methods for rarefied gas dynamics, preprint.
10. Pareschi L, Russo G. Asymptotic preserving Monte Carlo methods for the Boltzmann equation. *Transport Theory and Statistical Physics* 2000; **29**:415–430.
11. Pareschi L, Caflisch RE. Implicit Monte Carlo methods for rarefied gas dynamics I: the space homogeneous case. *Journal of Computational Physics* 1999; **154**:90–116.
12. Li Z-H, Zhang H-X. Numerical investigation from rarefied flow to continuum by solving the Boltzmann model equation. *International Journal for Numerical Methods in Fluids* 2003; **42**(4):361–382.
13. Pareschi L, Russo G. *An Introduction to Monte Carlo Methods for the Boltzmann Equation*. EDP Sciences. SMAI: 1999; 1–38.

14. Gabetta E, Pareschi L, Toscani G. Relaxation schemes for nonlinear kinetic equations. *SIAM Journal on Numerical Analysis* 1997; **34**:2168–2194.
15. Pullin DI. Direct simulation methods for compressible inviscid ideal gas flow. *Journal of Computational Physics* 1980; **34**:231–244.
16. Hash DB, Hassan HA. Assessment of schemes for coupling Monte Carlo and Navier–Stokes solution methods. *Journal of Thermophysics and Heat Transfer* 1996; **10**:242–249.
17. Bourgat JF, LeTallec P, Perthame B, Qiu Y. Coupling Boltzmann and Euler equations without overlapping. *Domain Decomposition Methods in Science and Engineering*, *Contemporary Mathematics*, vol. 157. AMS: Providence, RI, 1994; 377–398.
18. Bourgat JF, LeTallec P, Tidriri MD. Coupling Boltzmann and Navier–Stokes equations by friction. *Journal of Computational Physics* 1996; **127**(2):227–245.
19. LeTallec P, Mallinger F. Coupling Boltzmann and Navier–Stokes by half fluxes. *Journal of Computational Physics* 1997; **136**:51–67.
20. Garcia AL, Bell JB, Crutchfield WY, Alder BJ. Adaptive mesh and algorithm refinement using direct simulation Monte Carlo. *Journal of Computational Physics* 1999; **154**:134–155.
21. Wu J-S, Tseng K-C, Kuo C-H. The direct simulation Monte Carlo method using unstructured adaptive mesh and its application. *International Journal for Numerical Methods in Fluids* 2002; **38**(4):351–375.
22. Wild E. On Boltzmann's equation in the kinetic theory of gases. *Proceedings of the Cambridge Philosophical Society* 1951; **47**:602–609.
23. Carlen EA, Carvalho MC, Gabetta E. Central limit theorem for Maxwellian molecules and truncation of the Wild expansion. *Communications on Pure and Applied Mathematics* 2000; **53**:370–397.
24. Carlen EA, Salvarani F. On the optimal choice of coefficients in a truncated Wild sum and approximate solutions for the Kac equation. *Journal of Statistical Physics* 2002; **109**(1–2):261–277.
25. Hadjicostantinou NG. Analysis of discretization in the direct simulation Monte Carlo. *Physics of Fluids* 2000; **12**:2634–2638.
26. Pullin DI. Generation of normal variates with given sample. *Journal of Statistical Computation and Simulation* 1979; **9**:303–309.
27. Bourgat JF. Notice d'utilisation du logiciel BOL2D pour la simulation bidimensionnelle de l'equation de Boltzmann. *Rapport technique de l'INRIA-Rocquencourt*, *RT-0142*, 1992.

